Defence Research Establishment Pacific
Centre de recherches pour la défense pacifique

Technical Memorandum 90-14

EVALUATION OF ATTITUDE AND ACCELERATION SENSORS FOR MARINE APPLICATIONS

by

J.M. Preston

December 1990

DEFENCE RESEARCH ESTABLISHMENT PACIFIC
Research and Development Branch
Department of National Defence

Canada

Defence Research Establishment Pacific
Centre de recherches pour la défense pacifique

DEFENCE RESEARCH ESTABLISHMENT PACIFIC

CFB Esquimalt, FMO Victoria, B.C. VOS 1BO

Technical Memorandum 90-14

EVALUATION OF ATTITUDE AND ACCELERATION SENSORS FOR MARINE APPLICATIONS

by

J.M. Preston

December 1990

Approved by:

CHIEF

Research and Development Branch
Department of National Defence

Canada

ABSTRACT

A wide variety of instruments are available for measuring the attitude and accelerations of a marine vehicle, with characteristic advantages and limitations. The apparatus described here was built to evaluate such sensors against accurately measured accelerations and attitudes. It resembles a small Ferris wheel, and moves the sensor on 1.5-m diameter circles, on a support which remains horizontal, at selectable frequencies similar to those of ocean waves. The sensor can be yawed or pitched, asynchronously with the rotation. The acceleration and attitude of the sensor can be calculated from the shaft encoders on the rotation and yaw/pitch axles. Results are given for two inclinometers, an accelerometer, a piezoelectric angular-rate sensor, and a gyroscopically stabilized accelerometer package.

TABLE OF CONTENTS

LIST OF TABLES

INTRODUCTION

A wide variety of instruments and sensor packages are available for measuring the attitude and accelerations of a marine vehicle, from sophisticated gyroscopically stabilized accelerometers to simple pendulous inclinometers. Each type has characteristic advantages and limitations, of which some of the most important for marine vehicles are sensitivity, drift, frequency response, and immunity from motions or attitudes other than the one being measured. This memorandum describes an inexpensive apparatus built to measure these characteristics. Results are presented for two inclinometers, an accelerometer, a piezoelectric angular-rate sensor, and a gyroscopically stabilized accelerometer package. These results are presented to illustrate the tests possible on this apparatus, and also because these sensors are representative of motion-sensing instruments available today.

The apparatus can be pictured as a small Ferris wheel. The sensor under test is mounted on the sensor bracket, which is maintained horizontal by a chain mechanism. The sensor can be yawed or pitched, asynchronously with the rotation, at a rate determined by a second motor. Either yaw or pitch is selected by mounting the yaw/pitch platform horizontally or vertically on the sensor bracket. For calibration and for other measurements, the actual acceleration and attitude of the sensor are, of course, required. They can be calculated from the shaft encoders on the rotation and yaw/pitch axles.

Many sensor packages have been designed for aeronautical use, and have been thoroughly tested for that environment. However our literature searches have failed to identify any published reports on tests of sensors for wave-driven motion, which differs significantly in both frequencies and amplitudes. The apparatus described here was designed specifically to mimic ocean wave effects. Furthermore, low-drift-rate inertial navigation systems, are, in general, too expensive for most towed-body applications.

The apparatus was not designed to have the precision needed to test such systems.

There are several examples of towed bodies, ships, or associated equipment which use pendulous inclinometers to measure roll and pitch. It is well known that these results can be significantly contaminated by the acceleration of the sensor. Similarly, strap-down accelerometers do not measure just the accelerations of the body if the body pitches or yaws. This is discussed in this note, and some examples are presented.

Gyroscopically stabilized sensor packages are used, especially in research, to avoid these difficulties by keeping the accelerometers aligned with the true vertical or horizontal. While their performance is fully satisfactory for use in a towed body, as demonstrated by results obtained in this work, their high capital cost and maintenance requirements motivate a search for alternatives.

DESCRIPTION AND ANALYSIS OF SENSOR MOTION

The purpose of the rotating arm and the sensor bracket mounted on it is to simulate ocean-wave-driven motion in accurately known circumstances. The schematic drawing in Figure 1 shows the arm rotating about the X-axis, with radius R. The sensor table can be mounted horizontally or vertically on the bracket, rotating at the same radius, R. The bracket which supports the table is kept very nearly horizontal by a chain which connects a sprocket on the axle which supports the bracket to an identical stationary sprocket on the axis of rotation of the arm. Figure 2 shows the arm and its drive, and Figures 3 and 4 show the sensor table with various sensors mounted.

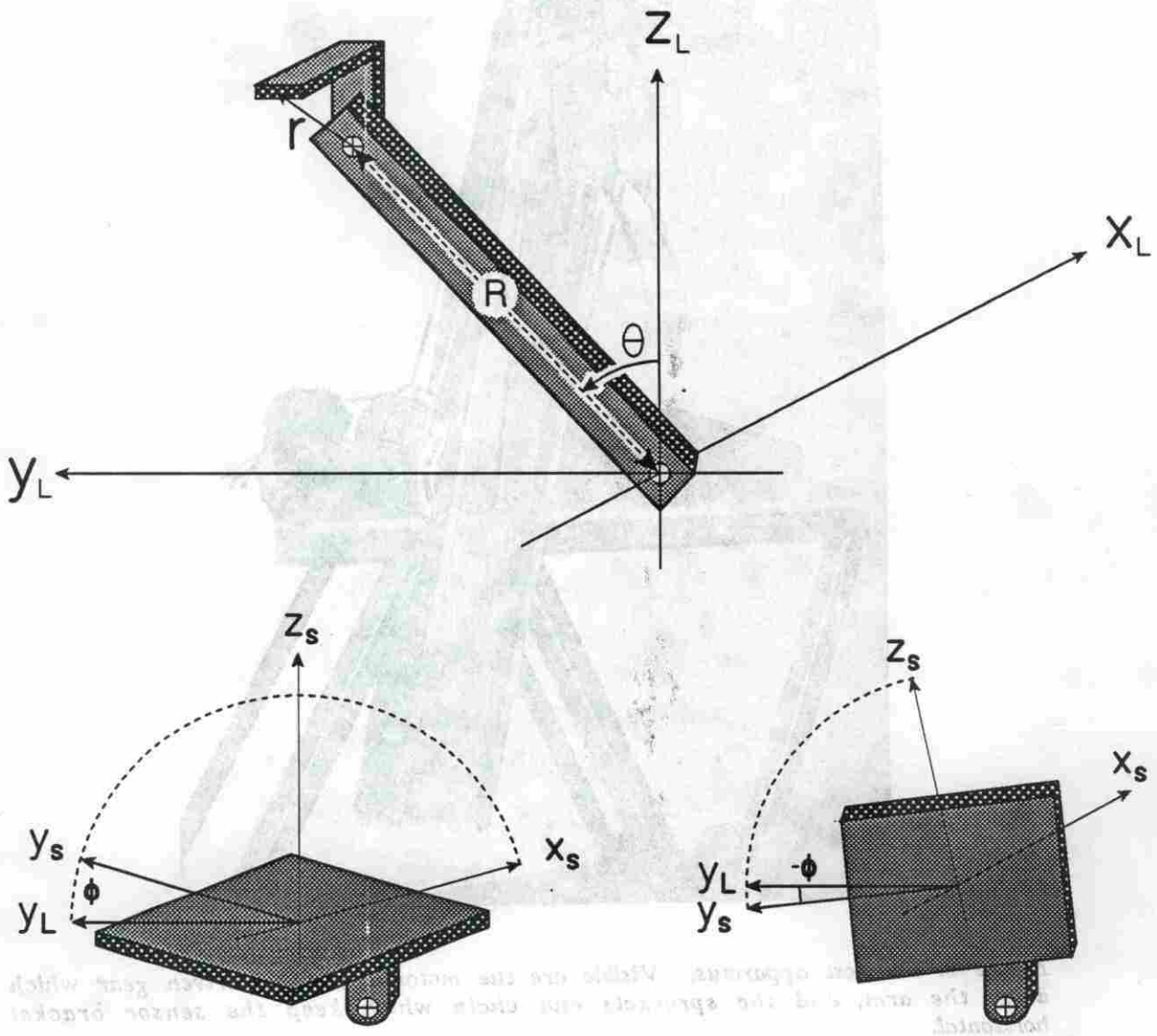

Horizontal Sensor Table

Vertical Sensor Table

Figure 1. The sensor table and arm, shown without the shafts and chain. The sensor table can be mounted horizontally, to simulate yaw by rotations about the z axis, or vertically, to simulate pitch by rotations about the x axis. Subscript L indicates the laboratory frame, S the sensor frame.

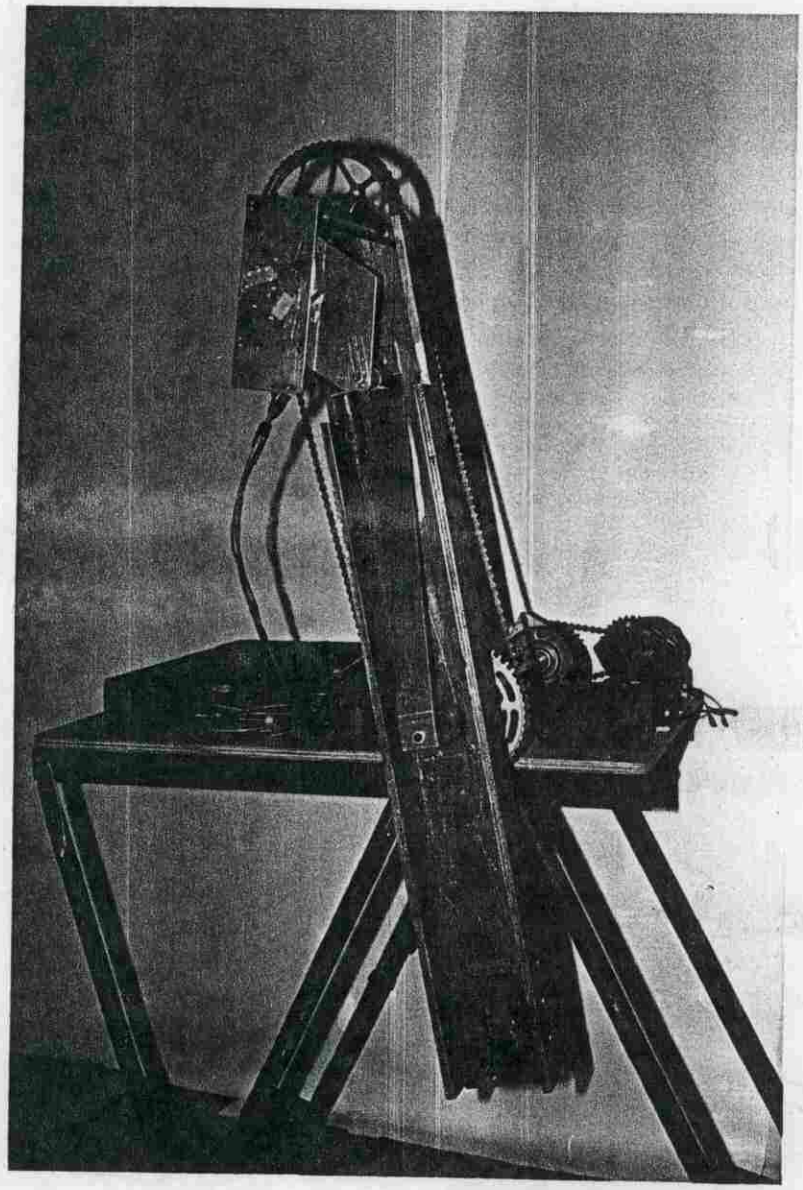

Figure 2. The test apparatus. Visible are the motor and chain-driven gear which drive the arm, and the sprockets and chain which keep the sensor bracket horizontal.

The arm is rotated by a variable-speed motor and a reduction gear, allowing periods of rotation from 7 to 16 s. Its radius is 0.752 m, thus the table speed ranges from 0.29 to 0.67 m/s. During a run this speed is kept constant, except for the small inherent variations discussed below. The position of the arm is measured by a synchro shaft encoder connected directly to the arm axle. These encoders, (Clifton Precision Products,

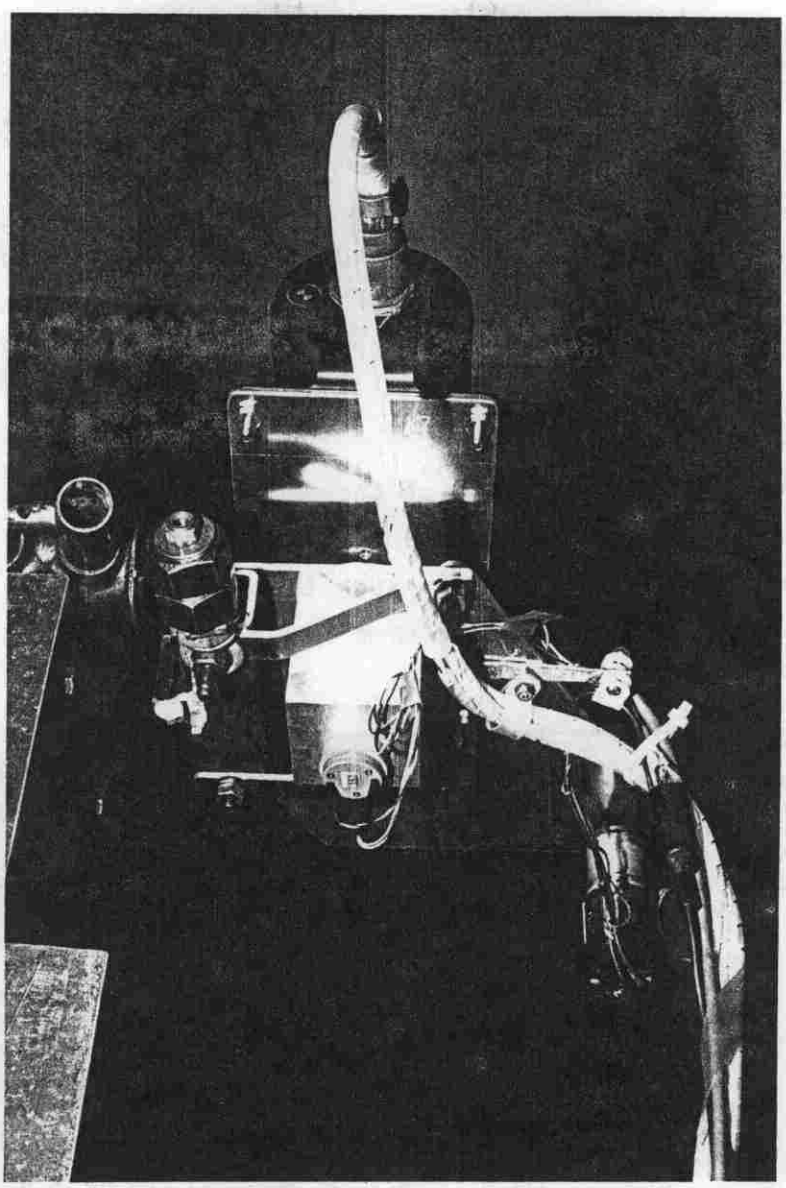

Figure 3. The sensor table, seen from below, with the Humphrey gyro-stabilized accelerometer package mounted for a test involving yaw. The yaw action was driven by the small motor on the bottom right, at an amplitude and mid-point selectable by moving pivots not visible in the picture. The shaft encoder can be seen, at the bottom end of the yaw axle.

Drexel Hill, Pa.) contain a stator with three windings and a single rotor winding, for the transmitter type used here, and sense rotation as the ratio of carrier amplitude across three terminals. They offer resolution of a few hundredths of a degree. This encoder was mounted such that its output was zero with the bracket-supporting axle directly above the arm axle.

The sensor table can be made to oscillate by a second variable-speed motor. Figures 3 and 4 show the mechanism which drives the oscillation. The amplitude can be adjusted by moving the pivot point along the slotted radial arm, and the table can be aligned to center the angular motion by moving a second pivot point along the slot in the table. When the table is mounted horizontally this oscillation is a yaw motion; when vertical it is a pitch motion. The angular position of the table is measured with an identical shaft encoder.

The oscillatory motion of the arm-driven table is not a simple sinusoid. A complete analysis of the motion of this linkage is lengthy and awkward. However the dimensions are such that the motion is very nearly a sinusoid, as shown by the power spectrum in Figure 5.

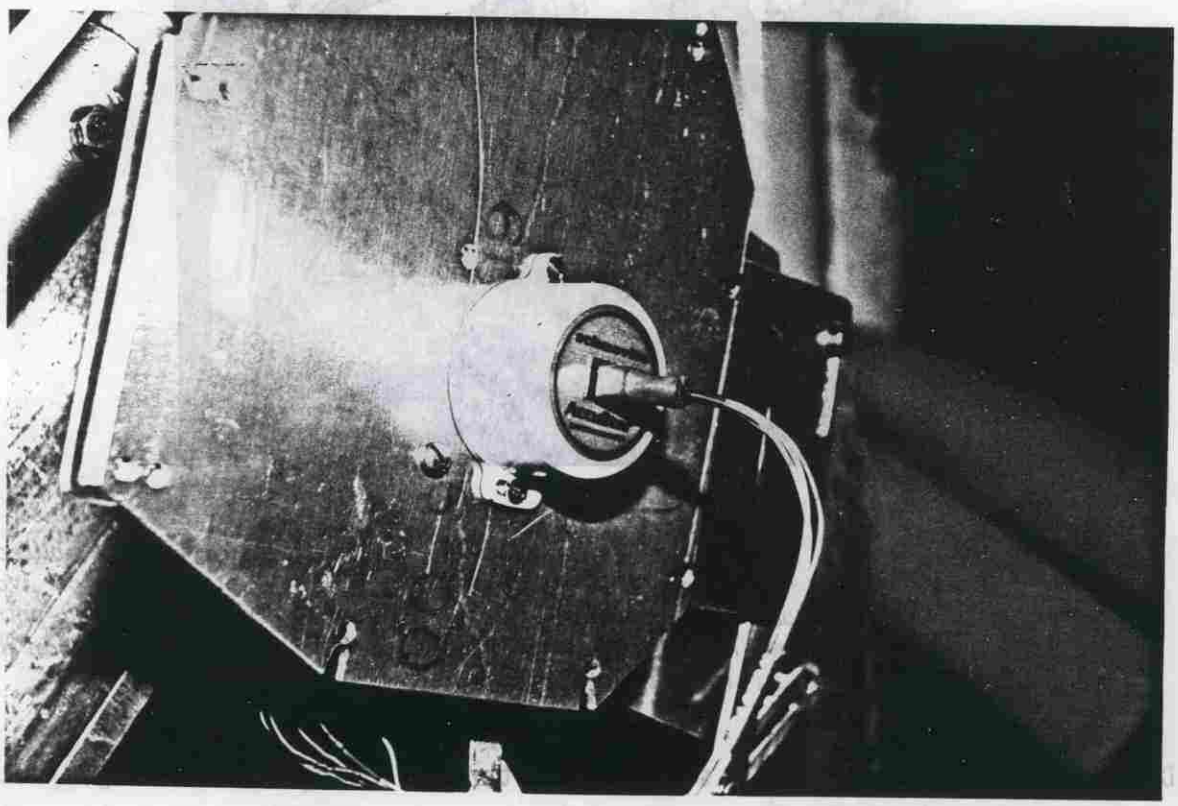

Figure 4. The sensor table, with a Schaevitz Accustar inclinometer mounted for a test involving pitch. Part of the linkage between the sensor table and the motor (shown in Figure 3) can be seen on the right.

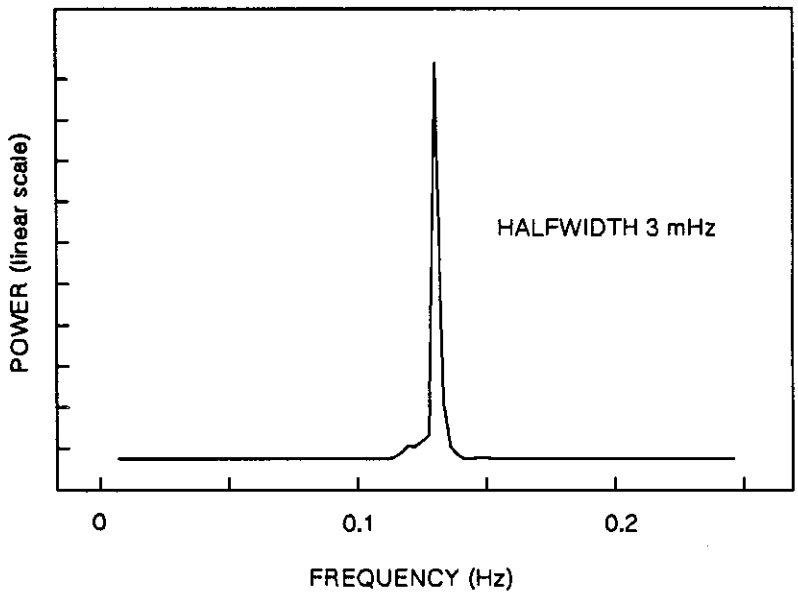

Figure 5. Typical power spectrum of the output of the shaft encoder which measures the oscillatory motion of the table. The centre frequency is determined by the voltage applied to the DC motor.

In actual waves, accelerations and attitude changes are, in general, synchronized in some way. However examples from References 1 and 2 show that the relationships between the various accelerations and angular motions are sufficiently complex that they may appear to be irregular. For this reason, this apparatus was designed with two independent drives. Data acquired over several periods of the difference frequency show the effects of all possible phase relationships.

Analysis of Table Motion

In preparation for evaluating and calibrating the performance of motion sensors, it was obviously necessary to analyze the motion of the table which carries the sensors. During an evaluation, the measured data were the angular positions of the arm and the table, as measured by the two shaft encoders, plus the data from the sensor itself. Thus procedures had

to be developed to calculate the detailed motion of the sensor table from the shaft-encoder data.

The coordinate system used in this analysis is shown in Figure 1. The arm rotates in the y-z plane, with the x-axis along its shaft and pointing from the arm toward the motor. The y-axis is to the left when looking along the x-axis and the z-axis points upward, thus the coordinate system is right-handed. Any sensor with a forward orientation, such as an accelerometer, was mounted with the forward direction along the positive y-axis. The sign conventions for angles are yaw positive to starboard, roll positive starboard up, and pitch positive bow up.

Rotation of the arm and the table employ the following variables:

θ	Arm	Angle from z axis
ω	Arm	Angular velocity
ϕ	Table	Angle from y axis (horizontal for yaw, vertical for pitch)
ν	Table	Angular velocity

Figure 1 illustrates these variables. Note that ϕ can have either of two meanings, depending on whether the sensor table was mounted horizontally or vertically.

If the apparatus were ideal, it would be elementary to calculate the motion of the sensor table from the measured angles, since both would be undergoing simple harmonic motion. The motion of the arm would move the table so that the coordinates of the sensor bracket, in the lab frame of Figure 1 with origin on the axis of rotation, would be:

$$\begin{bmatrix} x_L \\ y_L \\ z_L \end{bmatrix} = \begin{bmatrix} 0 \\ R\ \sin\theta \\ R\ \cos\theta \end{bmatrix} = \begin{bmatrix} 0 \\ R\ \sin\omega t \\ R\ \cos\omega t \end{bmatrix} \qquad (1)$$

The acceleration is the second derivative with time of Equation 1. The sensor reference frame (x_s, y_s, z_s) is, in general, either yawed or pitched by angle ϕ. Its acceleration is found by a coordinate transform, and is[1]

---

[1] The notation $\ddot{x}$ means d^2x/dt^2, and similarly for the other coordinates.

Yawing Sensor

$$\begin{bmatrix} \ddot{x}_s \\ \ddot{y}_s \\ \ddot{z}_s \end{bmatrix} = R\omega^2 \begin{bmatrix} \sin\theta \sin\phi \\ -\sin\theta \cos\phi \\ -\cos\theta \end{bmatrix} \qquad (2)$$

Pitching Sensor

$$\begin{bmatrix} \ddot{x}_s \\ \ddot{y}_s \\ \ddot{z}_s \end{bmatrix} = R\omega^2 \begin{bmatrix} 0 \\ \sin\theta \cos\phi + \cos\theta \sin\phi \\ -\sin\theta \sin\phi + \cos\theta \cos\phi \end{bmatrix} \qquad (3)$$

Equations 2 and 3 are accurate to a few percent in describing the motion of the sensor. However there were two other small effects which had to be considered before the apparatus could be used for calibration or for accurate evaluation. These were:

1. The sensor bracket undergoes incidental pitch, roll, and yaw because of various imperfections in bearings and shafts. These motions are distinct from the pitch or yaw imposed by the oscillating table.
2. The rotation frequency of the arm is not constant,

A major aim of the early work with the rig was to measure and characterize these incidental effects so they could be used in calculating the actual motion in later trials. First we describe the methods used to measure these incidental effects, and then we incorporate them into the equations of motion.

The incidental pitch, roll, and yaw of the sensor bracket, as functions of the arm angle θ, were measured in three ways.

1. A digital inclinometer, which had been zeroed against a carpenter's level with no observable end-for-end error, was used to measure roll and pitch with the arm stationary.
2. A He-Ne laser (eye-safe) was mounted on the table and the pattern it made on a large sheet of paper mounted on the wall 3.39 m away was recorded. By means of vertical and horizontal references on this paper, and also by noting the arm angle for each image point, the yaw and pitch as functions of arm angle could be calculated.

3. The Humphrey gyro-stabilized package measured pitch and roll.

The most accurate results were from the laser measurement. The paper tracing was a thin ellipse whose major axis was tilted from the vertical, due to incidental yaw. The laser beam followed the same path for each rotation of the arm. The maximum amplitudes of incidental pitch and yaw were found to be 0.15° and 0.45° respectively. The static inclinometer results were to an accuracy of $\pm 0.1^\circ$. The inclinometer and laser results for incidental pitch agreed, for the most part, to within that accuracy. Inclinometer results for incidental roll again showed a single cycle during each arm rotation, with a maximum amplitude of 0.7°. Results from the gyro-stabilized package, which were less accurate again, are discussed later.

These results indicated that the incidental pitch, roll, and yaw would be accurately described by nine parameters which, once measured, could then be used in all future trials. These parameters are the mean values, $\bar{\alpha}$, $\bar{\beta}$, $\bar{\gamma}$; amplitudes, α_o, β_o, γ_o; and phases, θ_α, θ_β, θ_γ, of the three angles:

$$\begin{array}{lll} \alpha & \text{yaw} & \alpha = \bar{\alpha} + \alpha_o \sin(\theta - \theta_\alpha) \\ \beta & \text{roll} & \beta = \bar{\beta} + \beta_o \sin(\theta - \theta_\beta) \\ \gamma & \text{pitch} & \gamma = \bar{\gamma} + \gamma_o \sin(\theta - \theta_\gamma) \end{array} \qquad (4)$$

The mean value of yaw, $\bar{\gamma}$, is more difficult to measure to our working accuracy, 0.1°, than the mean values of the vertical angles, which have a gravity reference. The technique we chose was to find that value of yaw which gave the smallest lateral acceleration as measured by the gyro-stabilized accelerometer package (without driving the oscillatory motion of the table). With the table mounted vertically, shims were added as necessary to null this acceleration; and with the table horizontal, thus the oscillatory motion being a yaw motion, the angle which minimized the lateral acceleration was taken as the centre for yaw.

All nine parameters were measured as described here, with results given in Table 1. Equation 4 was used to calculate the values of incidental yaw, roll, and pitch for any arm angle, θ, in any trial.

TABLE 1

PARAMETERS OF INCIDENTAL ANGULAR MOTIONS

	Mean		Amplitude	Phase
Sensor Table:	Horiz.	Vert.		
Yaw, α	0.0°	0.0°	0.47°	114°
Roll, β	-0.06°	0.15°	0.61°	-171°
Pitch, γ	-0.19°	-0.16°	0.12°	-21°

These incidental angular motions cause modest accelerations of the table. Although small, these accelerations should be calculated because they could be significant compared with the sensitivity of some sensors. Each of these angles was observed to undergo one cycle for each arm rotation, and thus they were believed to be due to varying tension in the chain. It seemed best to model these incidental pitch, roll, and yaw of the table as rotations about the shaft at the outer end of the chain, that is, the shaft which supports the 'dog-leg' sensor bracket (Figure 1). Let the vector from the centre of this shaft to the centre of the sensor be $\underline{r}$, with components $(r_x, 0, r_z)$. Since none of the angles exceed 1°, we can take $\sin(\alpha) = \alpha$ and $\cos(\alpha) = 1$ (also for β and γ) and we need not worry about the order of rotations in coordinate transformations. With the aid of the plans in Figure 6, the location of the centre of the table, in the laboratory frame, is found to be:

$$\begin{bmatrix} x \\ y \\ z \end{bmatrix} = \begin{bmatrix} -r_x - \beta\, r_z \\ R\,\sin\theta + \alpha\, r_x - \gamma\, r_z \\ R\,\cos\theta + r_z - \beta\, r_x \end{bmatrix} \qquad (5)$$

This equation reduces to Equation 1 if incidental yaw, pitch, and roll are ignored, except for a translation of the origin (which will vanish on dif-

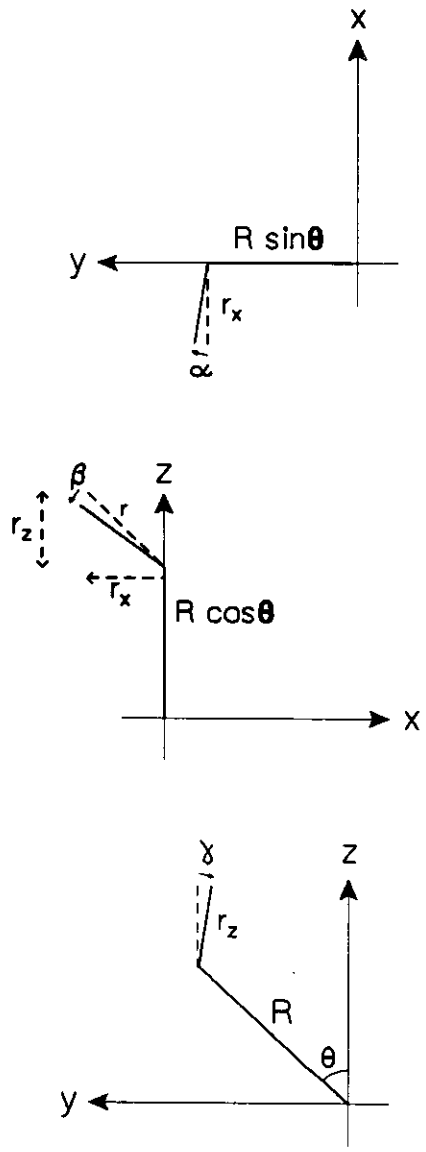

Figure 6. Projections of the arm and the strut which supports the sensor table.

ferentiation). The next step is to differentiate these equations twice to obtain accelerations, which will complete the consideration of the incidental angular motions. Before doing so, we will consider the second complication, variations in the rotation frequency of the arm.

The second complication is that the angular speed of the arm is not constant. Arm position, and thus angular speed, is, of course, measured at all times during each trial. In fact, angular speed varies not only with arm position (θ), but also from trial to trial because of imperfect balance of the arm (careful balancing was always done, but small differences remained). Calculations of table accelerations, then, could have been done by numerically differentiating the arm angle to obtain the angular velocity for any desired moment in any trial. However this process would have used only one arm-angle value and its immediate neighbours. Scatter in these data indicated that a better approach would be to use all the arm-angle-vs.-time data from the trial being analyzed, to derive an accurate angular velocity for each arm angle, θ. This was done by fitting the individual measurements of angular velocity as a function of arm angle to a Fourier series:

$$\omega = \omega_o \left[1 + \sum_{n=1}^{8} a_n \sin(n\theta) + b_n \cos(n\theta) \right] \tag{6}$$

where ω_o is the mean angular frequency, and a and b are the Fourier coefficients ($<<1$). Some useful expressions involving this series are:

$$\omega^2 = \omega_o^2 \left[1 + 2 \sum_{n=1}^{8} a_n \sin(n\theta) + b_n \cos(n\theta) \right] \tag{7}$$

$$\omega \frac{d\omega}{d\theta} = \omega_o^2 \left[\sum_{n=1}^{8} n\, a_n \cos(n\theta) - n\, b_n \sin(n\theta) \right] \tag{8}$$

The accelerations of the table, allowing for both complications, can now be found. In these expressions, second-order terms involving products of any of these angles and $d\omega/d\theta$, for example, were omitted since both terms are small.

$$\begin{aligned} \frac{dx}{dt} &= \frac{dx}{d\theta}\frac{d\theta}{dt} = \omega \frac{dx}{d\theta} \\ \frac{d^2x}{dt^2} &= \frac{d\theta}{dt}\frac{d}{d\theta}\left[\frac{dx}{dt}\right] = \omega \frac{d\omega}{d\theta}\frac{dx}{d\theta} + \omega^2 \frac{d^2x}{d\theta^2} \end{aligned} \tag{9}$$

and similarly for y and z.

The acceleration components of the sensor bracket in the laboratory frame, including the effects of both complications, are found from Equations 4, 5, and 9 to be:

$$
\begin{aligned}
d^2x/dt^2 &= r_z\,\omega^2\,\beta_o\,\sin(\theta - \theta_\beta) \\
d^2y/dt^2 &= -R\,\omega^2\,\sin\theta + R\,\omega\,\frac{d\omega}{d\theta}\cos\theta - r_x\,\omega^2\,\alpha_o\,\sin(\theta - \theta_\alpha) \\
&\qquad + r_z\,\omega^2\,\gamma_o\,\sin(\theta - \theta_\gamma) \\
d^2z/dt^2 &= -R\,\omega^2\,\cos\theta - R\,\omega\,\frac{d\omega}{d\theta}\sin\theta + r_x\,\omega^2\,\beta_o\,\sin(\theta - \theta_\beta)
\end{aligned}
\qquad (10)
$$

To apply these equations, the terms in ω are to be calculated using Equations 6-8.

The last step in the analysis is to transform the accelerations of the table to the coordinate system of the sensor. This is a straightforward coordinate transform using the yaw or pitch angle of the sensor, ϕ, the same as was done to obtain Equations 2 and 3 from Equation 1. As the results are rather lengthy, they will not be written here. However the comments in the macro "accs" have been carefully written and contain the full expressions.

Data Acquisition

As many as eight channels of analog data were filtered, amplified, and digitized during each trial. The filters had a corner frequency of 1.0 Hz and rolloff of 120 dB/decade. Each amplifier had separate offset and gain controls, which was very convenient but required detailed record keeping. Digitization was done at 3 Hz and was essentially simultaneous for all eight channels, although they were digitized in sequence, resulting in a serial data stream in RS-232 format.

The arm and table angles, from the synchro shaft encoders, were available in digital form, but were converted to analog voltages to facilitate recording and to ensure they were sampled simultaneously with the output(s) of the sensor. These voltages were simply connected as two channels of the eight-channel system.

The filter characteristics need to be considered in some detail, because the corner frequency is not much higher than frequencies of some of the motions. The 6-pole Butterworth filter has attenuation of 120 dB/decade above the corner frequency of 1.0 Hz. The phase-shift characteristics change steeply above about 0.2 Hz, and this delays our signals noticeably. However it is a very good approximation that the phase delay is proportional to frequency below 0.7 Hz. For nearly stationary signals, this means that the time delay is essentially constant. It turns out that this time delay is 0.64 s over the range 0.05 to 0.7 Hz, or very nearly two sampling periods, 2/3 s.

The values of arm angle increase from 0° to 360° at a nearly constant rate, and then fly back in about 20 ms. This rapid return caused ringing in the filter output. To avoid this, the filter was bypassed for this channel. Comparisons between the analog and sampled waveforms showed that aliasing was not occurring. However these data did not suffer a phase delay, and thus a delay had to be added to synchronize them with the other channels. As discussed above, this delay was very nearly two sampling periods for all arm rotation frequencies, 0.06 to 0.15 Hz, and thus was incorporated by a simple shift of the data.

While preparing for the trial, the data-gathering computer ran a program which demultiplexed the data stream, applied offsets and gains, and displayed each value under a user-selected heading. To conduct the trial, another program wrote the data streams as received at the communications port onto the hard disc, and a third program later demultiplexed these records and generated files, one for each data channel, suitable for plotting and calculation. These files were in integer form, so offsets and gains were still to be applied.

Calculation of Table Motion

The values recorded during a trial of a sensor are the two shaft angles and the sensor outputs. The aim of the calculations described here is to use the two shaft angles to calculate the angular motions and accelerations of the sensor, for comparison with the sensor outputs. They closely follow the theory outlined above and summarized in Equations 5-10.

These calculations were done primarily in the MAGnetics Interactive Graphics package, MAGIC, augmented with some FORTRAN programs. The FORTRAN programs worked only with the arm angle data. They corrected any values which happened to be digitized during the flyback, computed an average angular frequency for each arm position (specified within $\pm 1^{\circ}$) and for the run, and found the Fourier coefficients (Eq. 6). Further processing was done in MAGIC. For each sensor, a dedicated macro (e.g. "watson" or "schacc") read the data files of arm and table angles, and the Fourier coefficients, and converted the integral angle data to real values. Each macro also read the data from that sensor and applied the appropriate calibration and offsets for that sensor. These macros were similar, differing in the sensor calibrations and in some minor details of the setup of the apparatus. The lengthy macro "accs" then calculated yaw, pitch, roll and the three acceleration components in the sensor frame for both possible orientations of the table, and with and without gyro stabilization. Thus the detailed motion of the sensor table was calculated solely from the data from the shaft encoders.

Before presenting results, a comment on calibration constants, gains, and offsets is in order. Generally, the manufacturer's calibration constants were used, as the aim of this work was evaluation. Before a sea trial, obviously, this apparatus could be used to determine the best calibration values. Gains and offsets of the filter/amplifier cards were measured with DC voltages, and these results were used in the processing macros. The only exceptions are the acceleration data from the vertically stabilized package, for which the mean values over each trial were set to zero or g, as appropriate.

RESULTS

Introduction

In this section, the data from a sensor or sensor package is compared with values calculated as described above. The full calculation is difficult to understand because of the two complications, incidental attitude changes and non-constant arm rotation speed. If the motion is driven by the apparatus, the incidental effects are generally only a few percent and, to that accuracy, the motion is described by Equation 2 for a yaw motion or Equation 3 for a pitch motion. While these equations are useful to provide an intuitive understanding of the data, the plotted curves are always based on the full expressions. Some motions, though, would not occur in an ideal apparatus, and are classed as purely incidental. Table 2 lists these classes of motions.

TABLE 2

DRIVEN AND INCIDENTAL MOTIONS OF THE SENSOR TABLE

Table Orientation	Driven Motions		Incidental Motions
	Driven by Arm Alone	Driven by Arm and Table	
Horizontal	Vert	F/A Lat Yaw	Pitch Roll
Vertical	Vert* F/A*	Vert* F/A* Pitch	Lat Yaw Roll

* Vert, F/A, and Lat denote vertical, fore/aft, and lateral accelerations respectively. In the "Driven by Arm Alone" column, it is assumed that the sensor is aligned with the y axis. With the table vertical, and thus pitching when driven, vertical and fore/aft accelerations will be affected by the pitch unless a vertically stabilized (gyroscopic) package is used.

For any sensor evaluation or calibration, the trial would be selected to ensure that the sensor is being exercised by driven motions. The sensor pitch or yaw, as appropriate, would be, in those cases, simply the measured value of ϕ, and the pitch or yaw rate simply its derivative.

In this memorandum, though, there are some examples in which the incidental components are dominant. Examples are lateral acceleration with a pitching table, and roll under any circumstances. Some of these results are presented here as tests of our model of the incidental effects, others because they provide interesting insights into the behaviour of a sensor. Some physical insight into these incidental values can be obtained from Equations 4 and 10, but these equations are in the laboratory, not the sensor, frame.

Gyro-Stabilized Accelerometer Package

The SA09-0101-1 vertically stabilized accelerometer package, made by Humphrey Inc., San Diego, CA, measures vertical, fore-aft, and lateral acceleration from a gyroscopically stabilized platform. There are also gimbal pickoffs on the platform support which measure pitch and roll. DREP has used this package in previous towfish trials, but the work reported here was its first dynamic evaluation in highly controlled circumstances, except for factory calibrations. Since we regard this package as our "baseline" sensors against which others are evaluated, the results from this package are presented here in detail.

We consider, first, results with the oscillating table horizontal and thus producing yaw. The following examples are from a trial with ω = 0.740 rad/s, ν = 0.837 rad/s, and a yaw amplitude of 19.7°. Vertical acceleration is, to within a few percent, simply $-R\omega^2 \cos\theta$, (Equation 2) and Figure 7 shows excellent agreement indeed between the calculated and measured accelerations (calculated values reflect the full expression). Fore-aft acceleration has more complex time behaviour because the sensor package is being made to yaw, namely (Equation 2) $-R\omega^2 \sin\theta \cos\phi$ in simplified form. Figure 8 shows that agreement is still very good in this case.

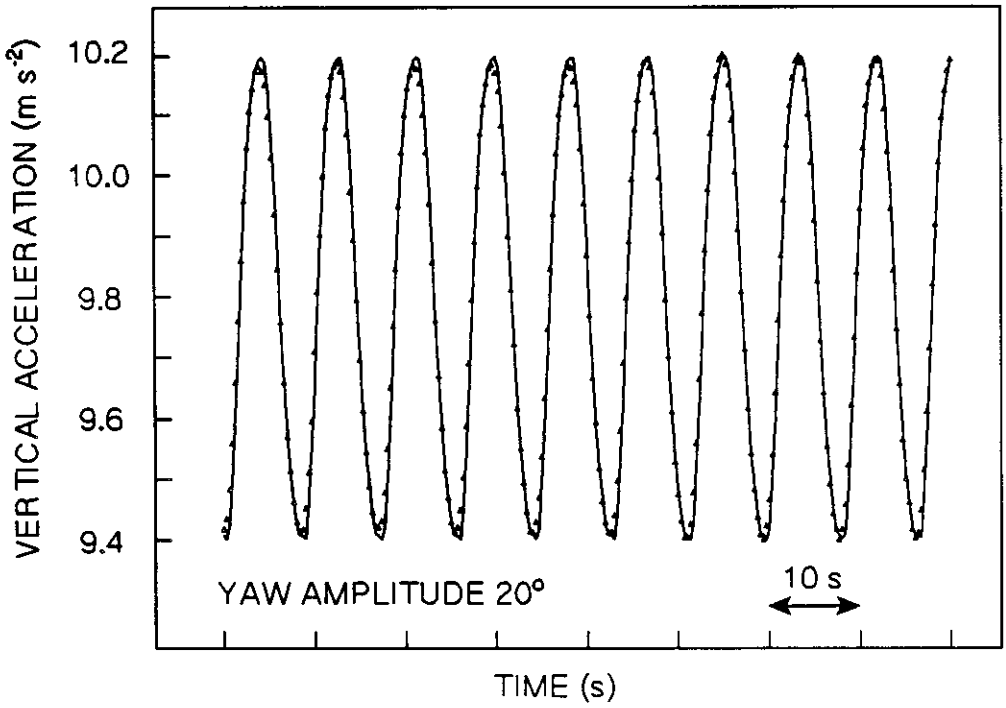

Figure 7. Vertical acceleration of the Humphrey gyro-stabilized accelerometer package as measured by that package (triangles) and as calculated from data supplied by the shaft encoders (curve). The trial conditions were arm rotation at 0.12 Hz and table yaw at 0.13 Hz.

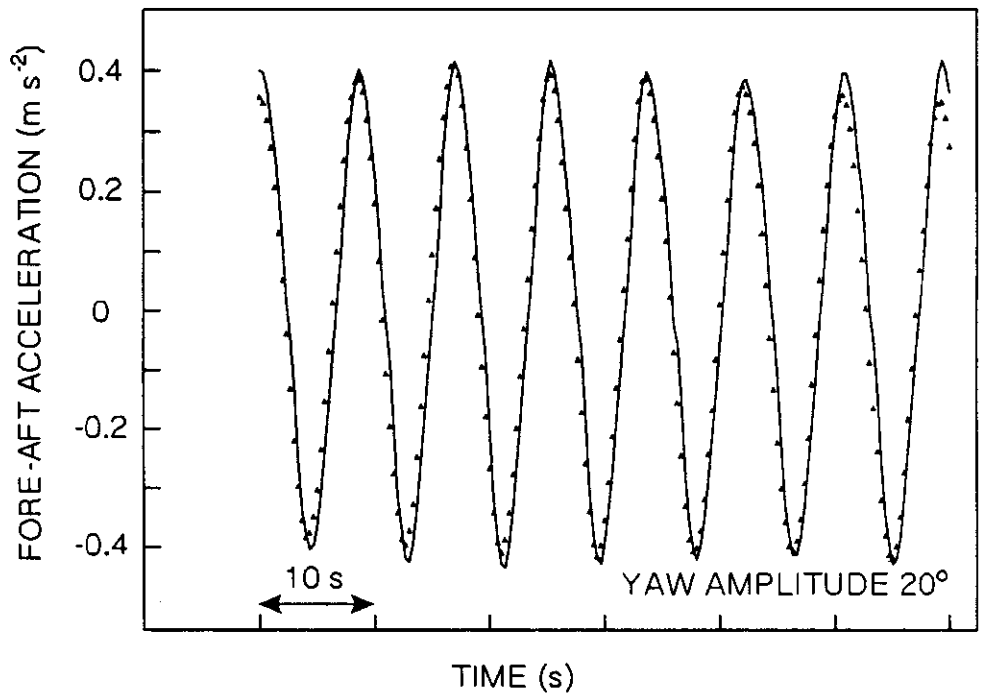

Figure 8. Fore-aft acceleration of the Humphrey gyro-stabilized accelerometer package as measured by that package (triangles) and as calculated from data supplied by the shaft encoders (curve). The trial conditions were arm rotation at 0.12 Hz and table yaw at 0.13 Hz.

The simplified expression for lateral acceleration in the sensor frame of reference (Equation 2) is $R\omega^2 \sin\theta \sin\phi$, which is far smaller than fore-aft acceleration since $\phi_{max} = 19.7°$. Some lateral acceleration data are shown in Figure 9, and the agreement can be seen to be about the same as with fore-aft acceleration, allowing for the difference in the scale of the plot. The complex pattern of lateral acceleration is due to beating of the arm-rotation and yaw frequencies. $R\omega^2 \sin\theta \sin\phi$ can be written

$$\frac{R\omega^2}{2}\left[\cos(\theta + \phi) - \cos(\theta - \phi)\right]$$

This elementary manipulation is demonstrated very clearly in Figure 10, which shows that the power spectrum consists almost entirely of the sum and difference frequencies, plus contributions from the primary frequencies due to the lesser terms.

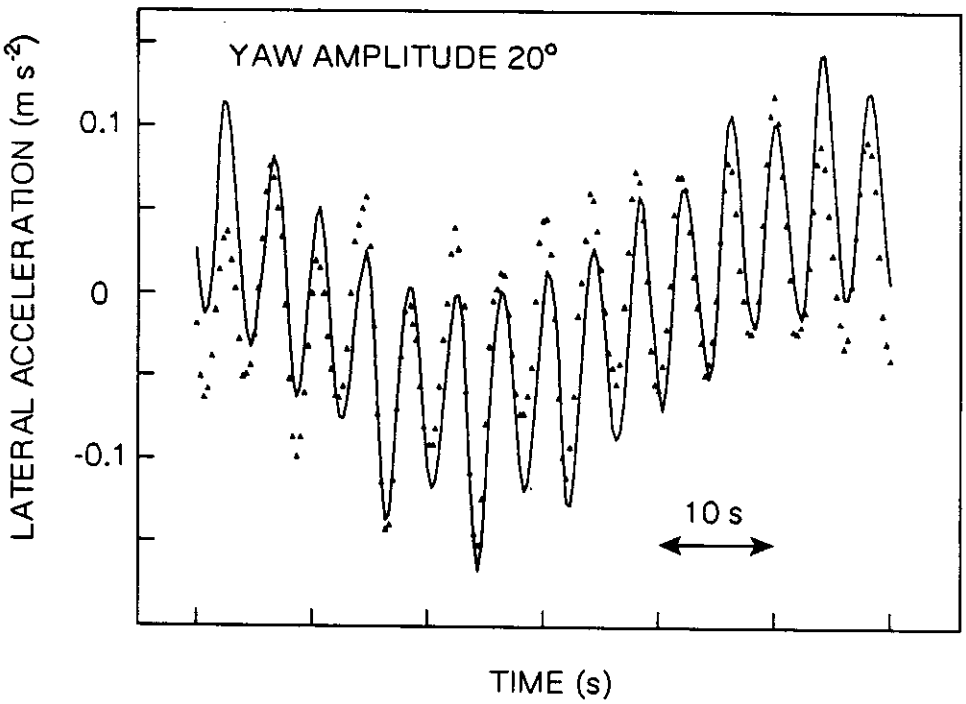

Figure 9. Lateral acceleration of the Humphrey gyro-stabilized accelerometer package as measured by that package (triangles) and as calculated from data supplied by the shaft encoders (curve). The trial conditions were arm rotation at 0.12 Hz and table yaw at 0.13 Hz.

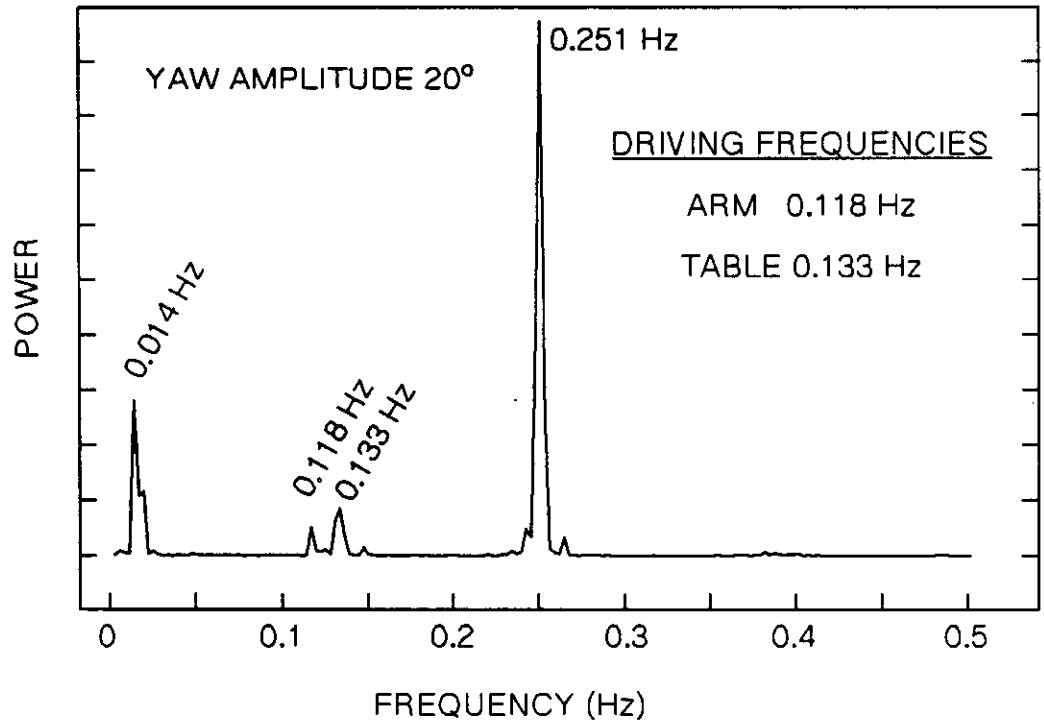

Figure 10. Power spectrum of the lateral acceleration of which a sample appears in the previous figure.

The beat phenomenon in which sum and difference frequencies are generated is present in many sensor measurements. Often other terms are important, which make it not as evident as it is here. Care must be taken to keep the sum frequency below about 0.7 Hz, to avoid undesirable distortion in the filters.

Pitch and roll, which are both incidental effects, are plotted in Figures 11 and 12. With pitch, agreement is within about 0.2°, equal to the manufacturer's claimed resolution. The roll data do not always agree even qualitatively, when theory is compared with the measurements. As this is more apparent in trials with the table vertical, it is discussed there.

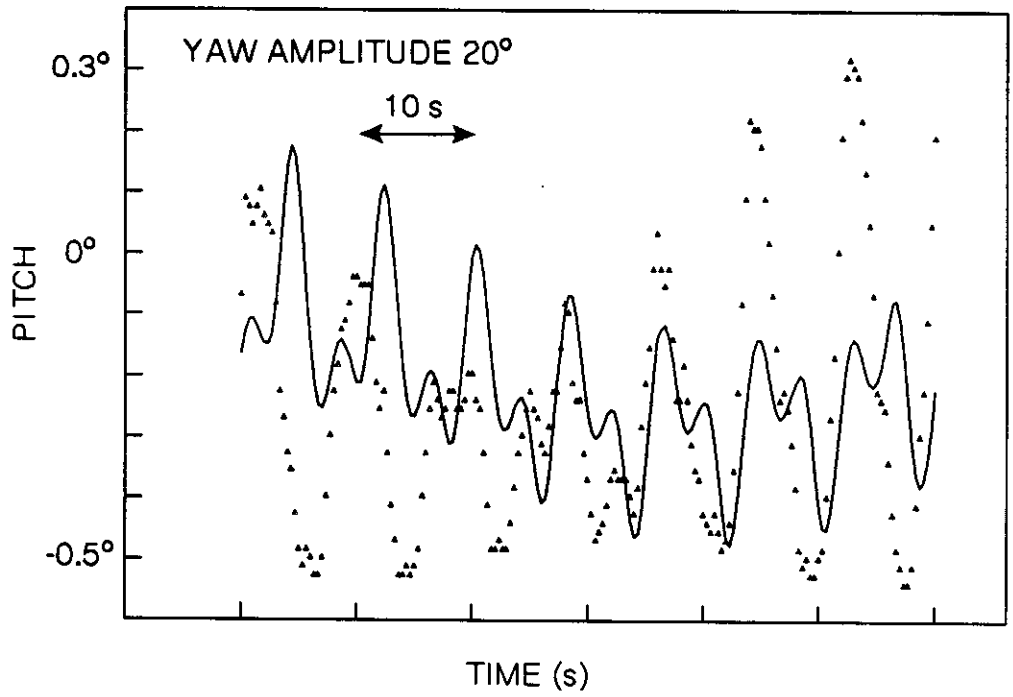

Figure 11. Pitch of the Humphrey gyro-stabilized accelerometer package as measured by that package (triangles) and as calculated from data supplied by the shaft encoders (curve). The trial conditions were arm rotation at 0.12 Hz and table yaw at 0.13 Hz.

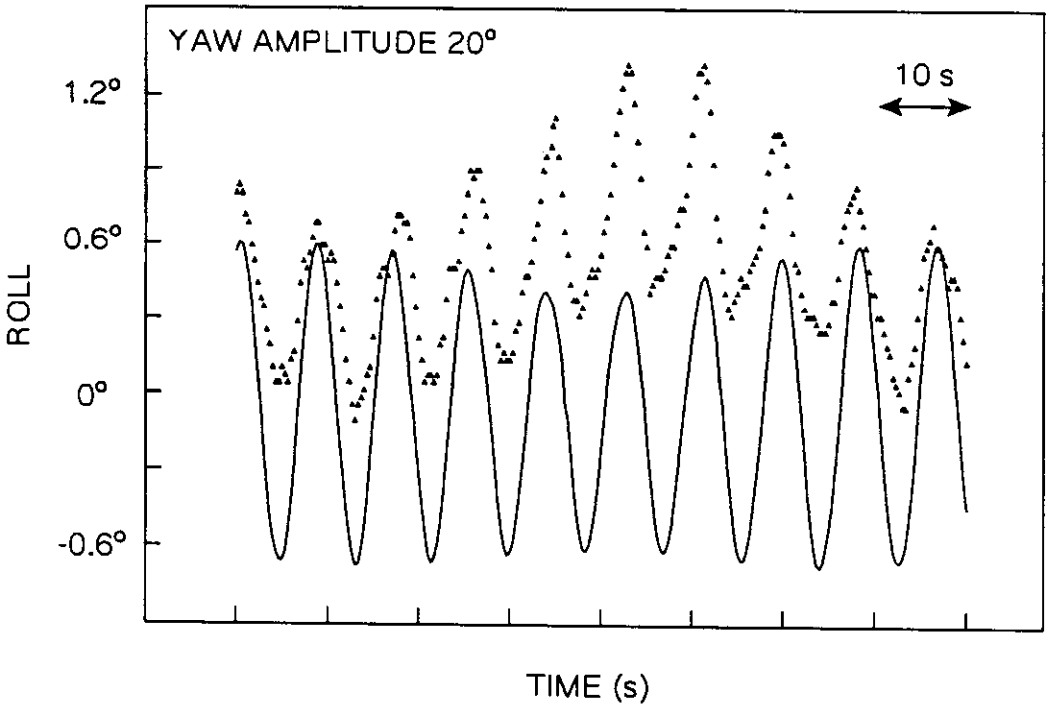

Figure 12. Roll of the Humphrey gyro-stabilized accelerometer package as measured by that package (triangles) and as calculated from data supplied by the shaft encoders (curve). The trial conditions were arm rotation at 0.12 Hz and table yaw at 0.13 Hz.

We will now examine results taken with the table vertical, that is, so that the driven oscillations of the sensor are a pitching motion.

With the table vertical, both the fore-aft and vertical accelerations, Figures 13 and 14, are driven by the pitching motion. In principle, the gyroscopic stabilization should remove the effect of pitch. The figures show that this is so, in that the recorded data is of essentially constant amplitude. The predicted and measured values of pitch, Figure 15, also agree well. The discrepancy in this figure appears to be mostly a small error in establishing the offset, as the mean values disagree by a constant value of about 1°. Angular data were not adjusted in the data processing to bring mean values into agreement.

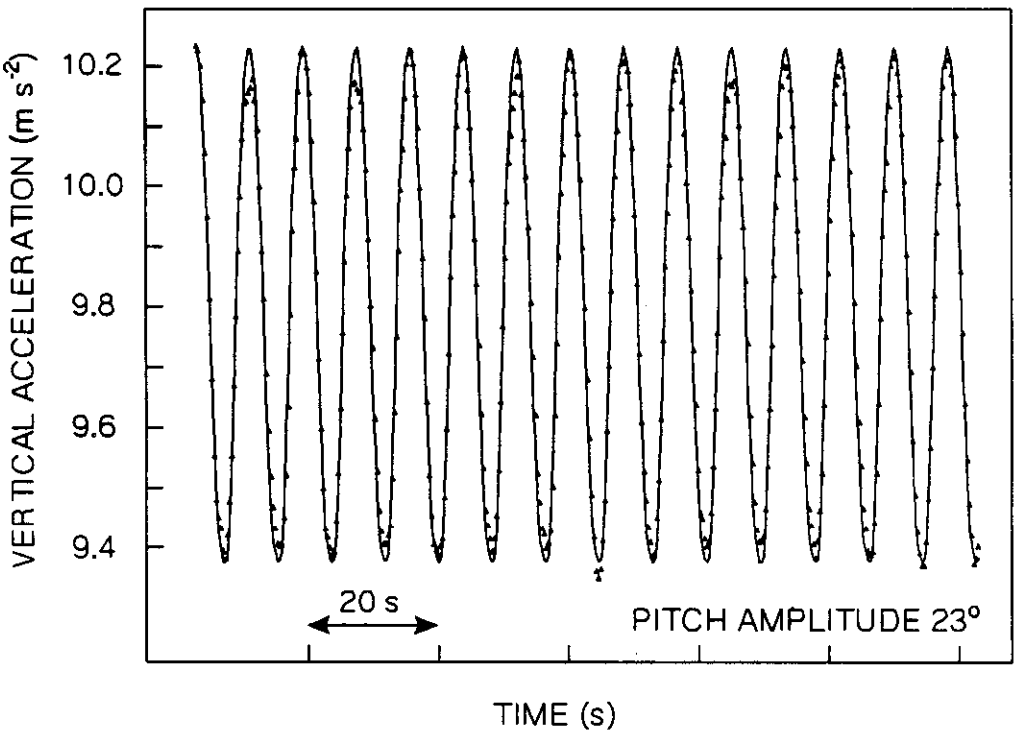

Figure 13. Vertical acceleration of the Humphrey gyro-stabilized accelerometer package as measured by that package (triangles) and as calculated from data supplied by the shaft encoders (curve). The trial conditions were arm rotation at 0.12 Hz and table pitch at 0.16 Hz.

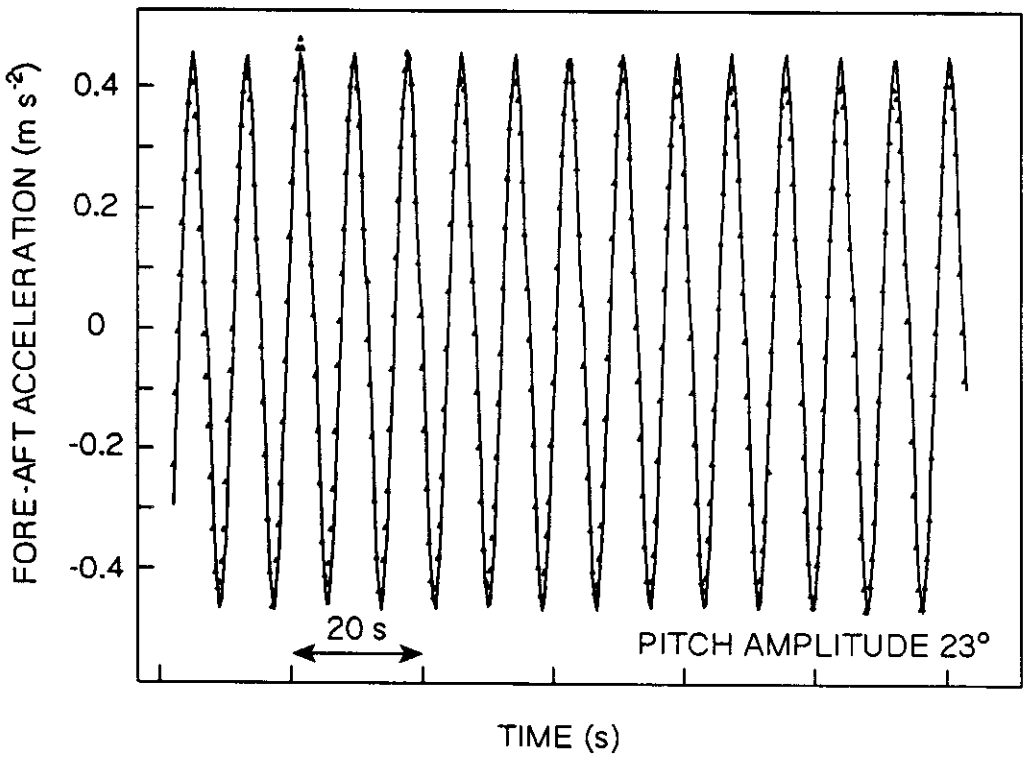

Figure 14. Fore-aft acceleration of the Humphrey gyro-stabilized accelerometer package as measured by that package (triangles) and as calculated from data supplied by the shaft encoders (curve). The trial conditions were arm rotation at 0.12 Hz and table pitch at 0.16 Hz.

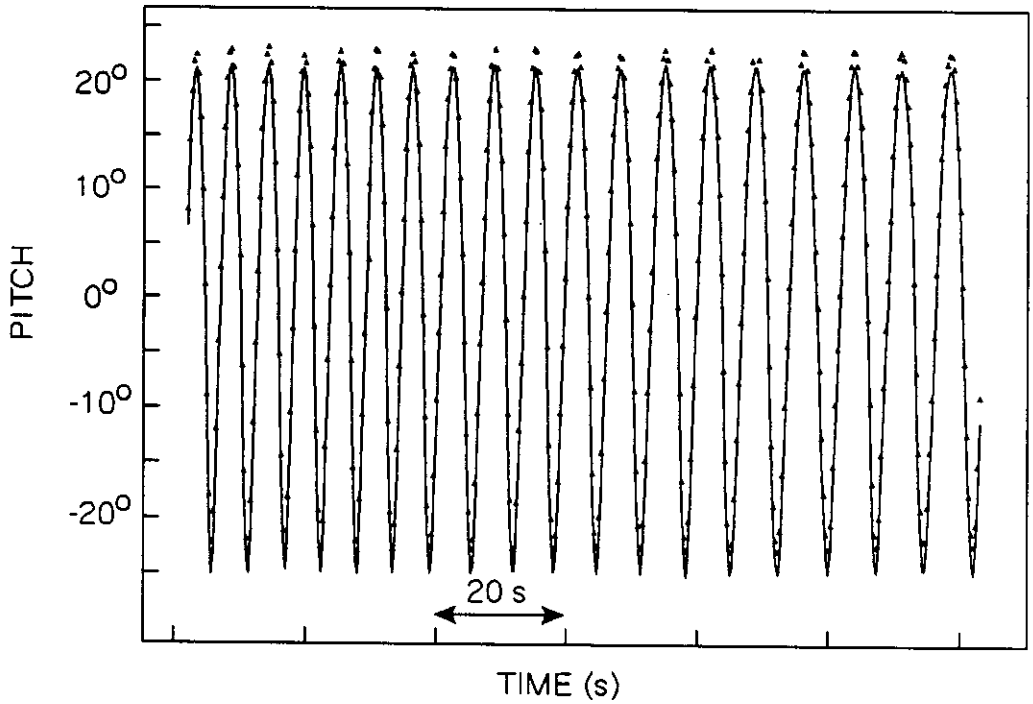

Figure 15. Pitch of the Humphrey gyro-stabilized accelerometer package as measured by that package (triangles) and as calculated from data supplied by the shaft encoders (curve). The trial conditions were arm rotation at 0.12 Hz and table pitch at 0.16 Hz.

The incidental motions with this geometry, namely roll and lateral acceleration, are small and thus reveal the performance limits of this package. The plot of roll, Figure 16, shows that the output does not completely follow the incidental roll as calculated from Equation 1. These discrepancies are not inconsistent with the manufacturer's claimed resolution of 0.2°. In other words, the vertical reference of the sensor package can be 0.2° or so off the true vertical.

The measured values of lateral acceleration, Figure 17, show a consequence of this resolution limit. The theoretical acceleration due to incidental roll is extremely small, far less than the measured acceleration. What causes the observed acceleration? It can be seen to be uncorrelated with arm rotation, since the theoretical acceleration is at that frequency. It was found to be strongly correlated with the pitch angle, which is proportional to the larger curve shown in that figure. And how does the pitch

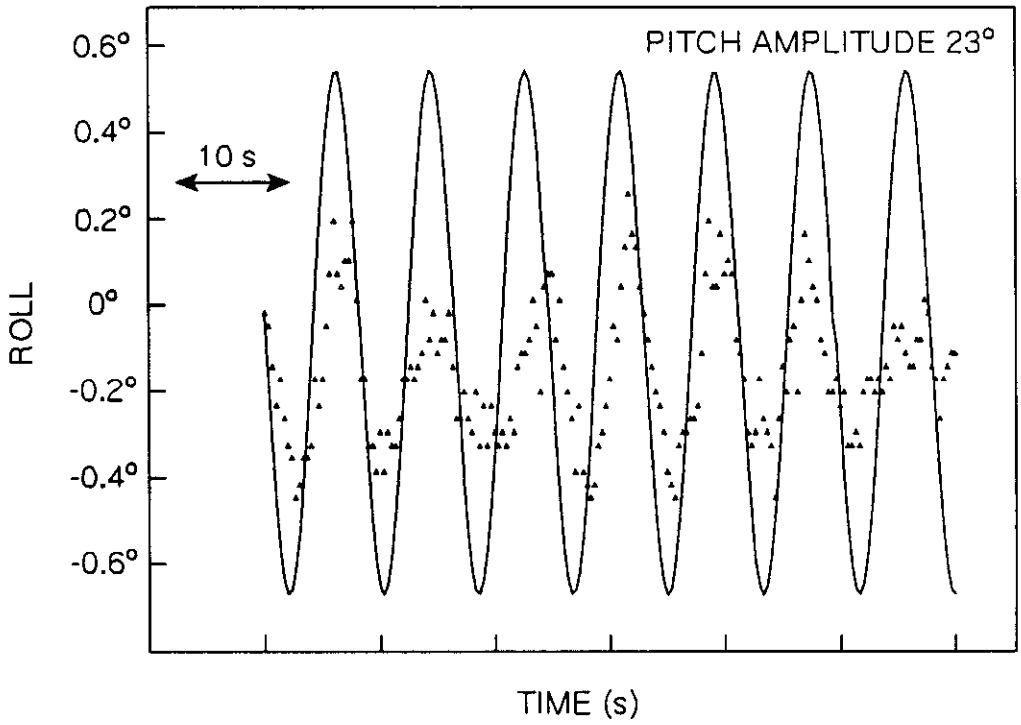

Figure 16. Roll of the Humphrey gyro-stabilized accelerometer package as measured by that package (triangles) and as calculated from data supplied by the shaft encoders (curve). The trial conditions were arm rotation at 0.12 Hz and table pitch at 0.16 Hz.

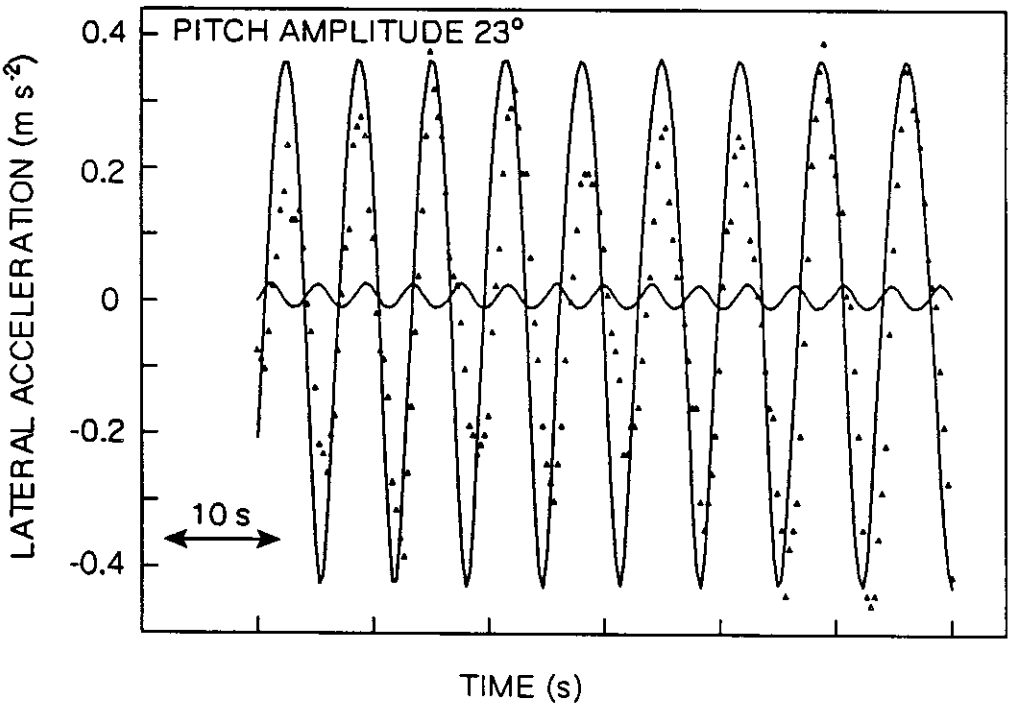

Figure 17. Lateral acceleration of the Humphrey gyro-stabilized accelerometer package as measured by that package (triangles) and as calculated from data supplied by the shaft encoders (small-amplitude curve). The large-amplitude curve is pitch angle (degrees)/585. The trial conditions were arm rotation at 0.12 Hz and table pitch at 0.16 Hz.

angle cause lateral acceleration? It cannot be a matter of pitch causing small yaw angles and introducing a component of fore-aft acceleration, because fore-aft acceleration is sinusoidal about zero at the arm-rotation frequency, which would destroy the strong observed correlation for at least some cycles. Thus it must be that pitch produces small amounts of roll, which cause a component of gravity to appear as lateral acceleration. Suppose that the pitching action introduces roll equal to 1% of the pitch. The maximum roll would be 0.2°, and we have seen that this is too small to be compensated by the vertical stabilization. The resulting lateral acceleration, in m s^{-2}, would then be $1\% \times \phi \times 9.8 \times \pi/180 = \phi/585$ (ϕ is the pitch angle in degrees). A plot of $\phi/585$ appears in the figure and can be seen to agree reasonably well with the observations. This appears to be an interesting example of the resolution limits of the vertical stabilization and of its effects on acceleration outputs.

This example shows that the resolution of the vertical stabilization was about 0.2°, and that an accelerometer oriented at this angle to the vertical would be subject to a gravitational component of 0.03 m s^{-2}. This value is similar to the sensitivity quoted by the manufacturer of the accelerometer, and thus should be regarded as the acceleration sensitivity of the package.

All trials at frequencies similar to or higher than the examples given above showed at least as good agreement between theory and measurement by the gyro-stabilized package, except for occasional trials in which one accelerometer briefly gave unreasonable results.

Piezoelectric Angular Rate Sensor

This rate sensor is a "tuning fork" device designed to sense angular rates accurately while rejecting accelerations. As this ability is normally found only in gyroscopic devices, these sensors are of considerable interest due to their modest cost and power consumption. A sensor was evaluated in this work for accuracy in measuring rates and for rejection of acceleration parallel and perpendicular to the sensing axis.

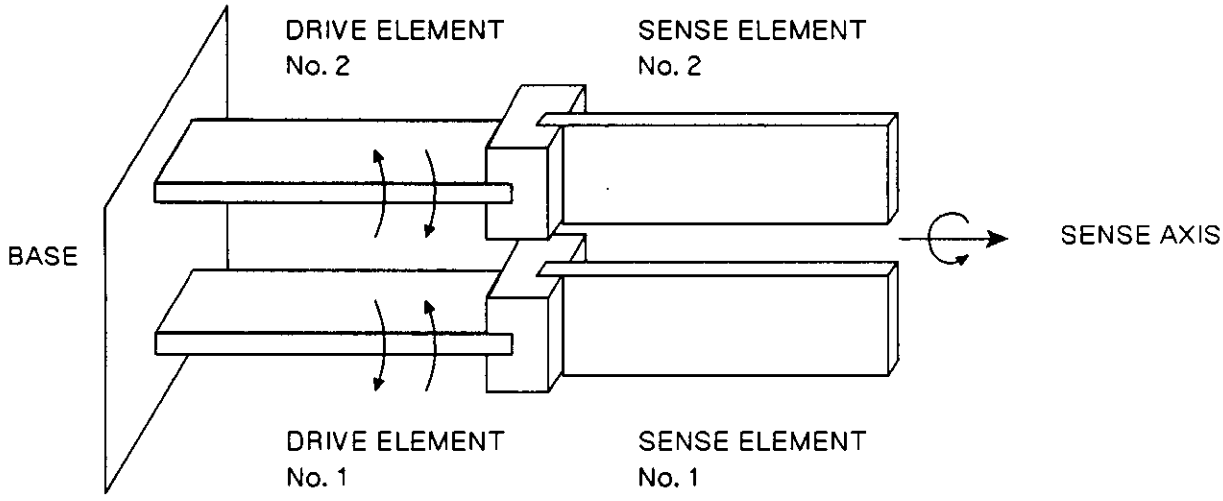

Figure 18. Schematic diagram of the piezoelectric transducer elements in the Watson angular rate sensor (patent pending).

The operating principle (patent pending) of these sensors can be described with reference to Figure 18. The piezoelectric drive elements each move a piezoelectric sensing element in a reciprocating arc. Any bending of the sensing elements, caused by accelerations, produces a voltage across their electrodes. In particular, rotation about the sense axis causes Coriolis acceleration, and thus a signal proportional to angular rate. The two elements are driven 180° out of phase, which creates a nodal plane for mounting and a cancellation of common accelerations, thereby largely eliminating, in theory, the effects of external vibrations and accelerations.

Figure 19 shows the results from a trial of this sensor (Watson ARS-C121-1A, 30°/s full scale, Watson Industries Inc., Eau Claire, WI). The sensor was mounted on the horizontal table, which was driven to yaw as the

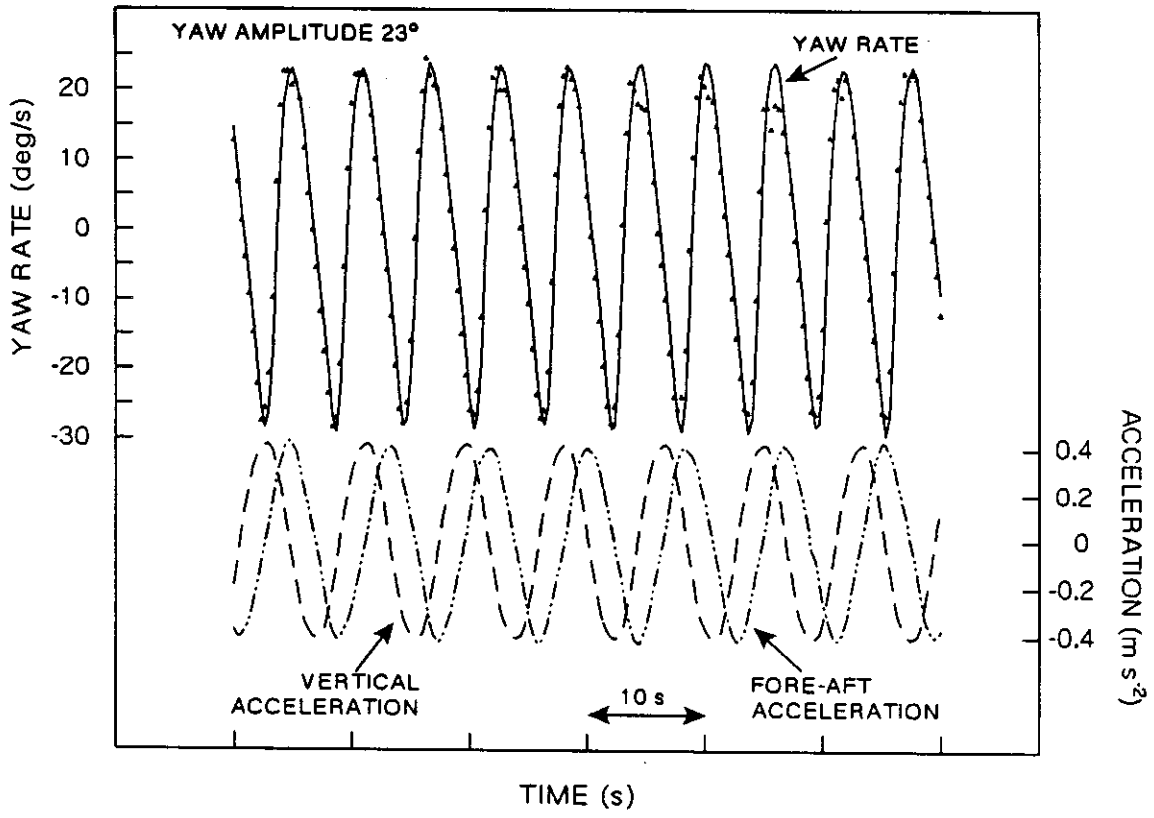

Figure 19. Yaw rate (left-hand scale) of the Watson angular rate sensor, during accelerations, as calculated from the shaft encoders (solid line) and as measured by the sensor (triangles). Also shown are the accelerations which the sensor was undergoing (dashed lines, right-hand scale). The trial conditions were arm rotation at 0.12 Hz and sensor yaw at 0.17 Hz.

arm rotated. The sense axis was vertical, coincident with the yaw axis, and the rotating arm caused vertical and fore-aft accelerations. As with all the sensors, the values recorded during the trial were the two shaft-encoder outputs and the data from the sensor. The two angle measurements were processed in the macros "watson" and "accs" to calculate the actual accelerations and attitudes of the sensor, as described above. The figure shows good agreement between the actual yaw rate and the measurement by the Watson sensor. The calibration constant used to plot the sensor results was 3.18°/s/V, rather than 3°/s/V as specified by the manufacturer.

The yaw rate measurements do not seem to be affected by the accelerations plotted in the figure, since there do not appear to be any correlations between disagreements in the rate measurement and the magnitude of either acceleration. This can be shown very clearly because the yaw and the accelerations are at different frequencies. The power spectra of acceleration and of yaw rate are shown in Figure 20. The main peaks of each are at

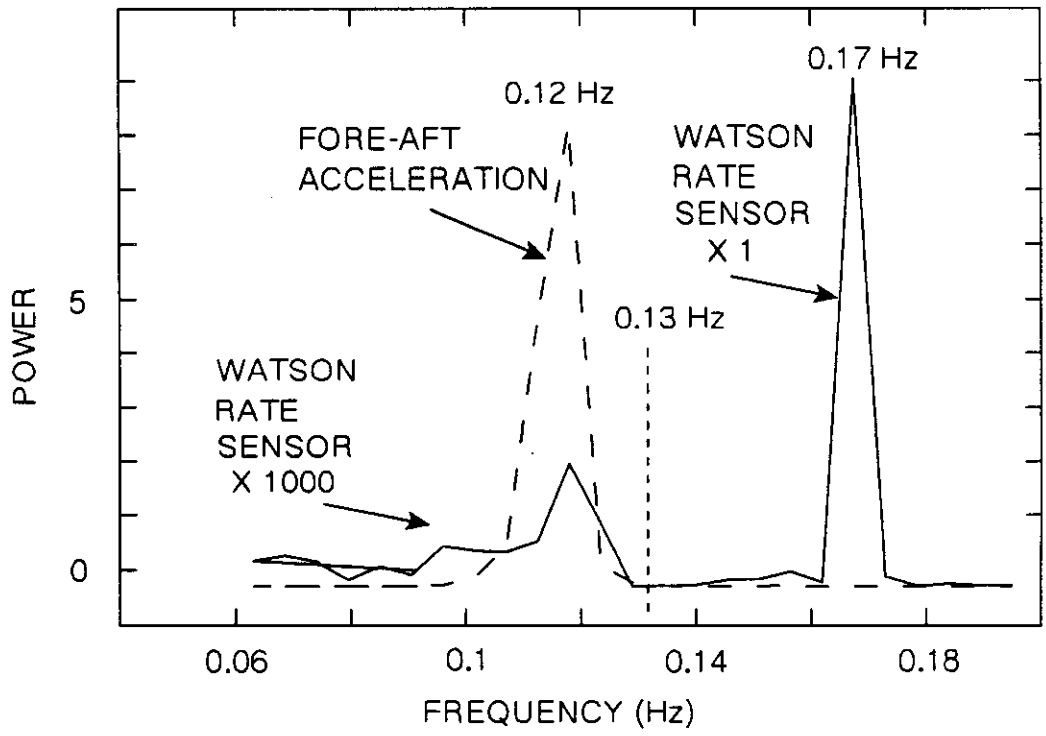

Figure 20. Power spectra of the yaw rate as measured by the Watson rate sensor and of its fore-aft acceleration, for the trial shown in the previous figure. The scale factor of the rate-sensor power spectrum is 1000 times larger below 0.132 Hz.

the frequencies of arm rotation, ω = 0.758 rad/s (0.12 Hz), and table yaw, ν = 1.06 rad/s (0.17 Hz), respectively. (Equation 2 shows that the fore-aft acceleration depends on $\sin\theta$ ($\theta=\omega t$) and on $\cos\phi$ ($\phi=\nu t$), but the ϕ dependence is less important because $\phi<23^\circ$.) The purpose of the figure is to search for any output from the rate sensor at the frequency, ω, at which it was being accelerated. Since none whatsoever could be seen on the initial plots, the scale factor of the rate-sensor power spectrum was increased by 1000 below 0.132 Hz, producing the modest peak shown. We conclude that for typical wave-driven motion, accelerations of the sensor cause less than one part per thousand of the measured angular rate.

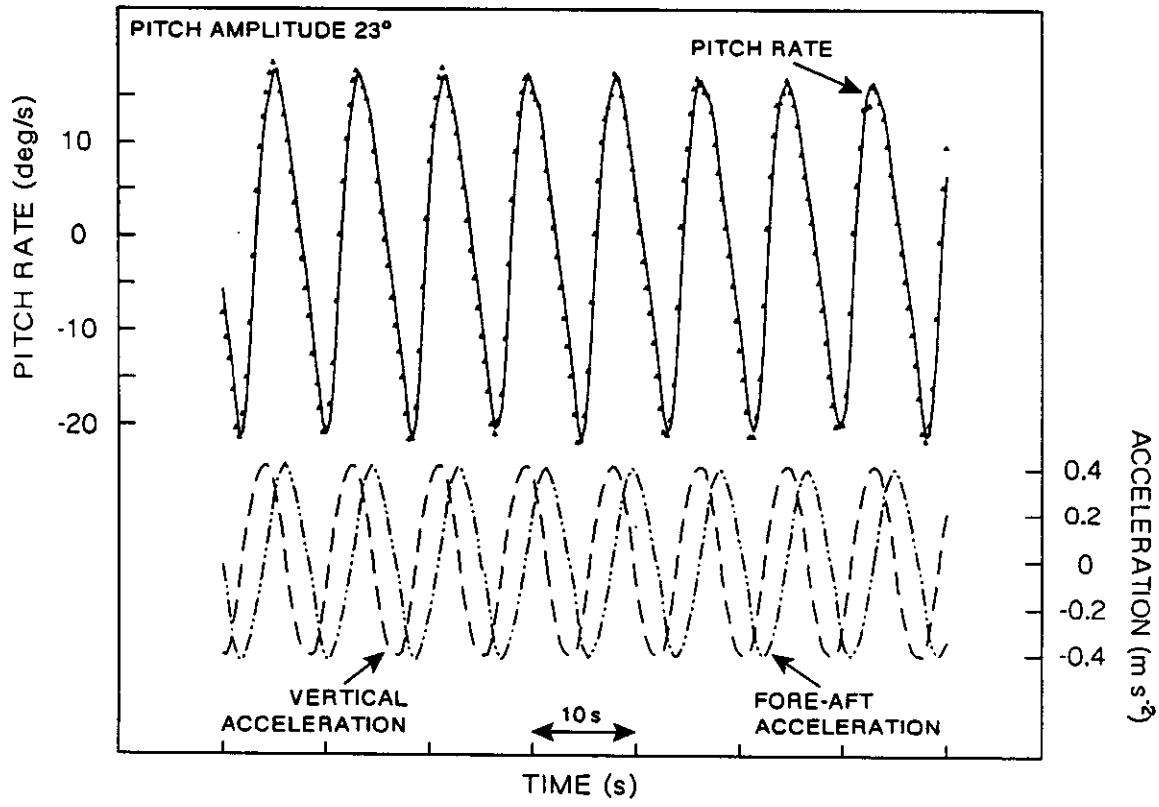

Figure 21. Pitch rate (left-hand scale) of the Watson angular rate sensor, during accelerations, as calculated from the shaft encoders (solid line) and as measured by the sensor (triangles). Also shown are the accelerations which the sensor was undergoing (dashed line, right-hand scale). The trial conditions were arm rotation and sensor yaw both at 0.12 Hz.

Similar results were obtained with the table vertical and thereby pitching, rather than yawing, the sensor. In this configuration, the sense axis was athwartships, and both the significant accelerations were transverse to it. Figure 21 again shows excellent agreement between the calculated and measured pitch rates, with no observable effect due to accelerations. In this trial, the frequencies were too similar to separate the effects by examining power spectra.

Inclinometers and Accelerometers

Two inclinometers and an accelerometer were tested on this apparatus with several purposes in mind:

1. Assess the accuracy of these sensors, as they are representative of sensors of these types.
2. Demonstrate the errors which can arise from treating the data from these sensors as if they were stabilized.
3. Demonstrate that the resonant frequency of the sensor must be significantly higher than wave frequencies.

Each sensor was mounted on the vertical table and subjected to simultaneous pitch and acceleration. The accelerometer was also evaluated on the yawing table, also while being accelerated.

Strapdown accelerometers do not indicate true acceleration unless the body is horizontal. Also, inclinometers do not indicate true attitude if the body accelerates. Depending on the application, the design of sensor packages could ignore this effect, or locate the accelerometers on a gyroscopically stabilized platform, or measure attitude by some other means and correct the accelerometer outputs. The first option introduces errors which are often unacceptable, as illustrated below. The second option is the basis of many commercial packages and inertial navigation sensors. One example is the Humphrey sensor package analyzed in this work, in which the accelerometers are on the stabilized platform, and the pitch and roll are angles between that platform and reference directions on the casing. The third option is attracting increasing commercial attention now that it is

practical to integrate the output of angular rate sensors accurately. These rate sensors could be of the piezoelectric type evaluated here, while for inertial-navigation systems they are likely to be ring-laser or fibre-optic gyros.

Most accelerometers, including the one evaluated here, measure force applied to a test mass which is usually constrained to move along a line. Provided the line remains horizontal, a component of the true acceleration is measured. In general, though, the body has non-zero pitch or roll, thus the line is not horizontal, and thus a component of gravity also acts on the test mass.

Humphrey CP17-0601-1 Inclinometer

This economical standard pendulum is a purely mechanical device which measures the angle from vertical by means of a potentiometer pickoff. Its natural frequency is 3.2 Hz, with damping of 0.3. Accuracy is therefore determined by constraints on mechanical motion and by the precision of the potentiometer and of the voltage applied to it.

Figures 22 and 23 compare the pitch as measured by the inclinometer with the true pitch of the sensor plus the contribution from acceleration. No "after-the-fact" constants have been used here - the gain of the filter/ amplifier was measured statically and the calibration of the inclinometer was simply that 15.0 V was applied to the 90° potentiometer. The agreement could hardly be better.

These figures also illustrate the difference between pitch measured by the inclinometer, I, and the true pitch ϕ. The true pitch, obtained directly from the shaft encoder output, is not shown directly on the figures as it would have obscured the data. It consisted of near-sinusoids with very similar zero crossings and phase, and of regular amplitude bounded by the dashed lines. The observed maximum differences between I and ϕ were about 4.5° (with $\omega \simeq 1$ rad/s and a radius of 0.75 m, the maximum fore-aft

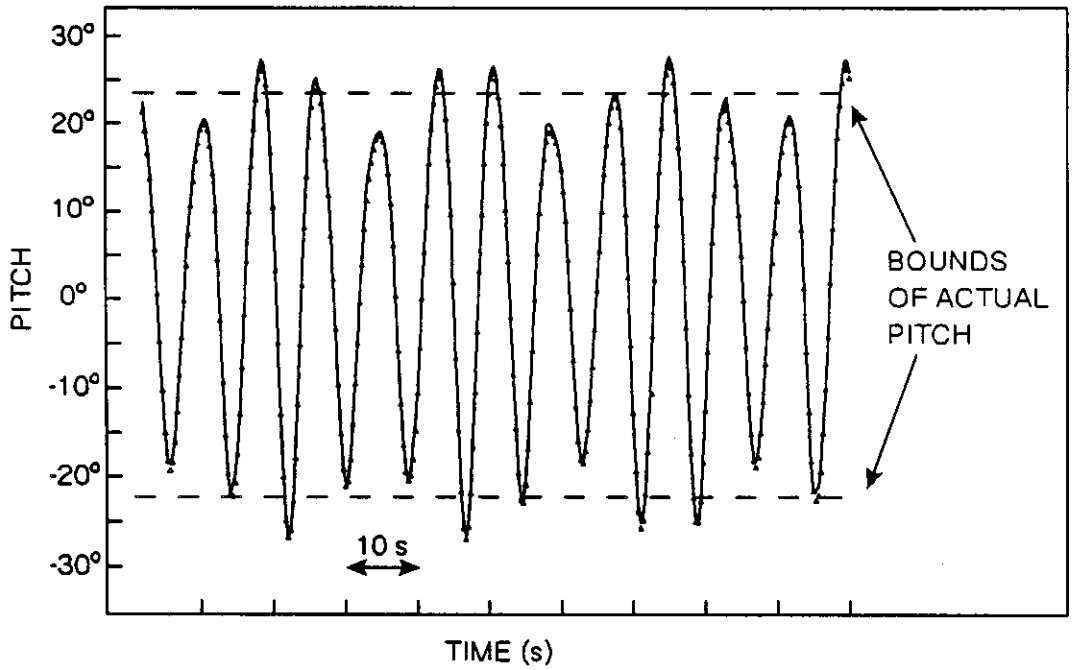

Figure 22. Pitch as measured by the Humphrey inclinometer (triangles) from a trial with the arm rotating at 0.16 Hz and the table pitching at 0.12 Hz. The solid curve is the output one would expect from an inclinometer, allowing for the fore-aft acceleration of the sensor. The dashed lines indicate the maximum amplitude of the true pitch.

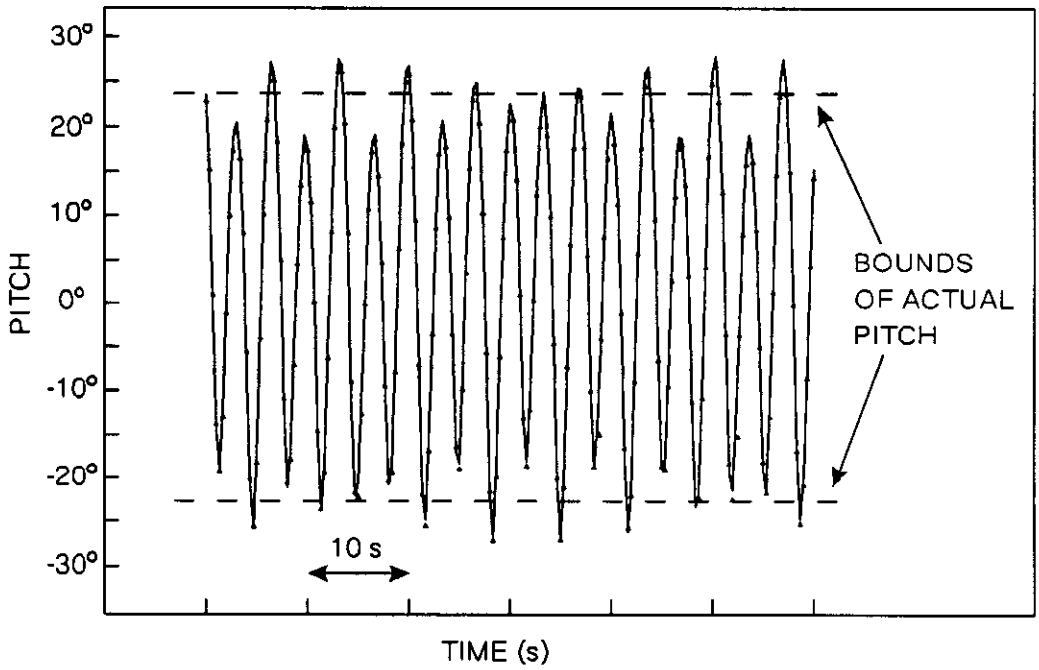

Figure 23. Pitch as measured by the Humphrey inclinometer (triangles) from a trial with the arm rotating at 0.16 Hz and the table pitching at 0.30 Hz. The solid curve is the output one would expect from an inclinometer, allowing for the fore-aft acceleration of the sensor. The dashed lines indicate the maximum amplitude of the true pitch.

acceleration was 0.75 m/s^2, and $\tan^{-1}(0.75/9.8) = 4.4°$). This difference can be taken as typical for wave-driven motion.

Schaevitz "Accustar" Inclinometer

This inclinometer is an electronic device which senses inclination through gravitational effects on a pair of capacitors. The manufacturers (Schaevitz Sensing Systems, Phoenix, AZ.) do not disclose further details of the design. The claimed resolution is 0.001°. Like most inclinometers, it is compact and inexpensive.

Figures 24, 25, and 26 compare its output with the actual pitch, as measured by the shaft encoder. These graphs are similar to those presented above, for the Humphrey inclinometer. In particular, the deviations from true pitch due to acceleration of the sensor are essentially identical.

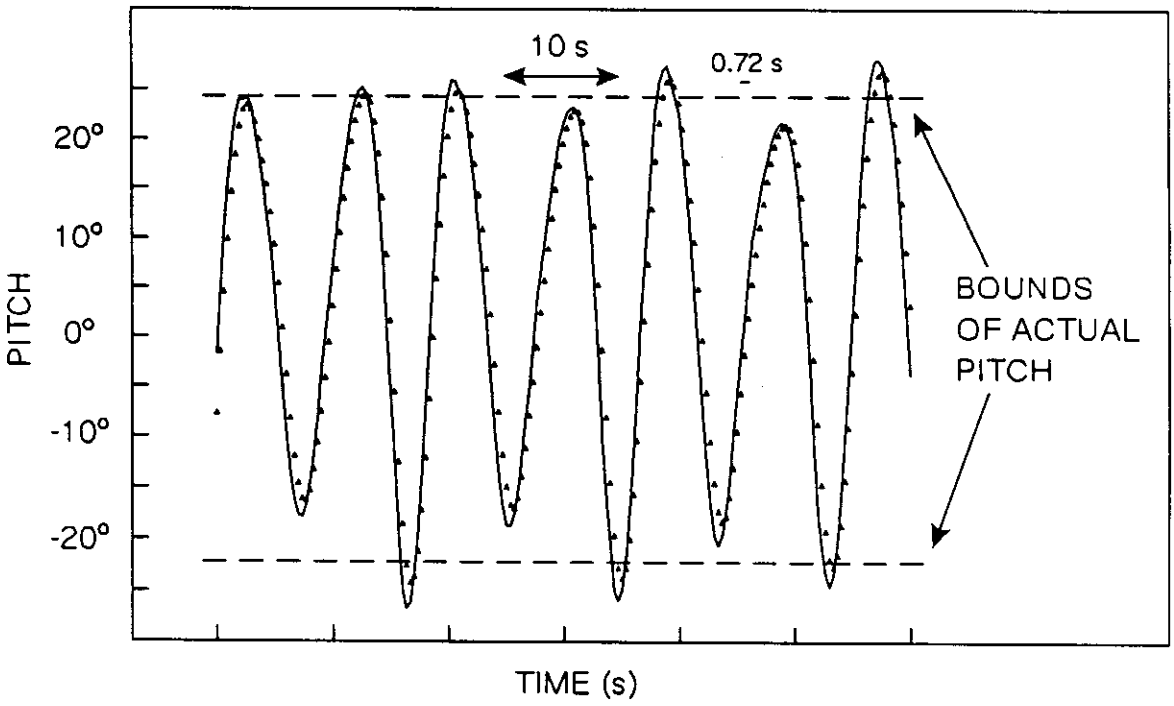

Figure 24. Pitch as measured by the Schaevitz inclinometer (triangles) from a trial with the arm rotating at 0.16 Hz and the table pitching at 0.11 Hz. The solid curve is the output one would expect from an inclinometer, allowing for the fore-aft acceleration of the sensor. The dashed lines indicate the maximum amplitude of the true pitch. The line 0.72 s long indicates the theoretical delay due to mechanical damping in the inclinometer.

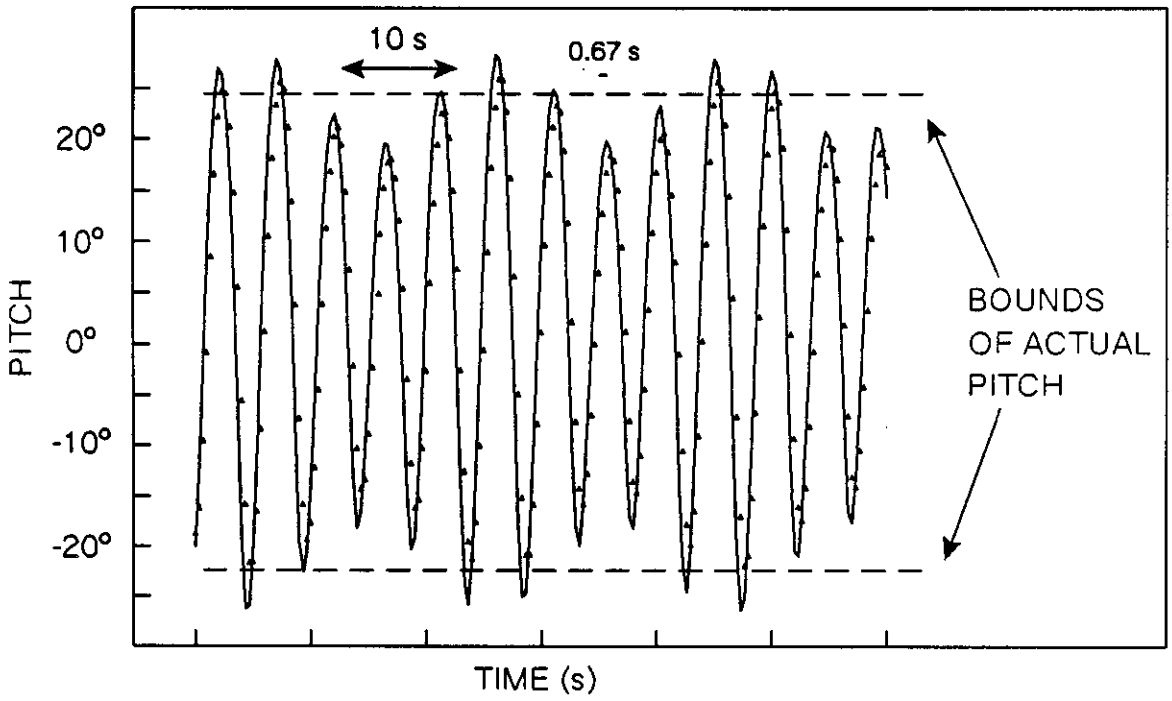

Figure 25. Pitch as measured by the Schaevitz inclinometer (triangles) from a trial with the arm rotating at 0.16 Hz and the table pitching at 0.21 Hz. Curves, dashes, and the line 0.67 s long have the same significance as in the previous figure.

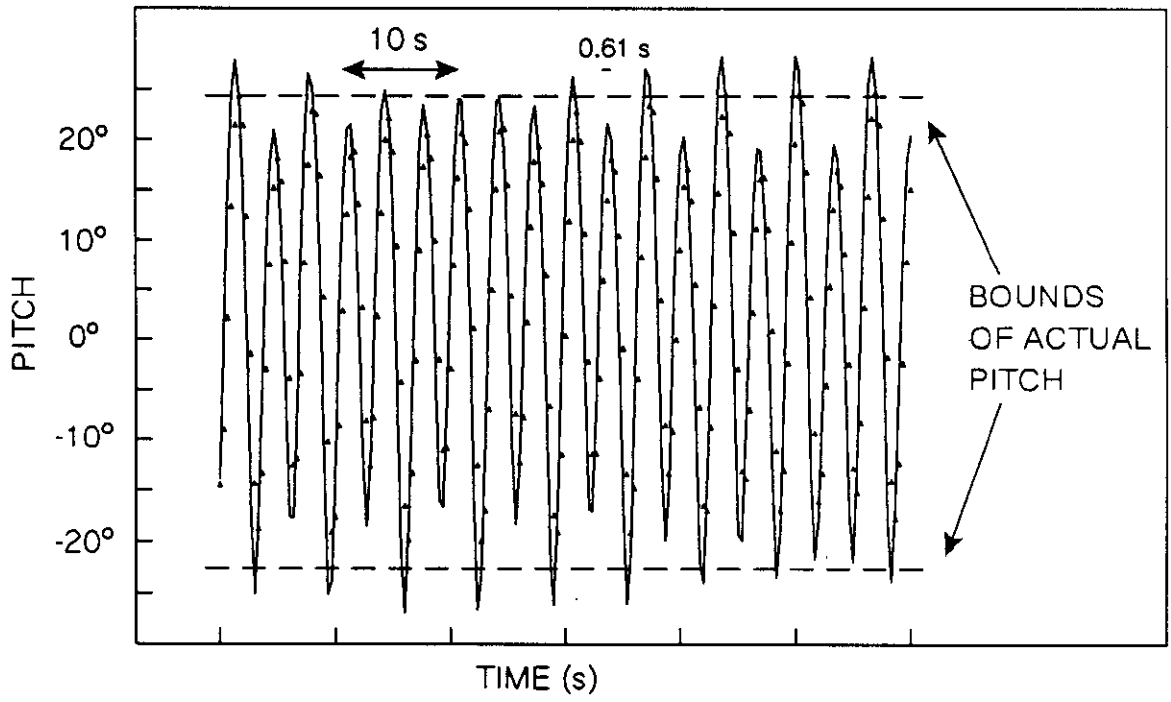

Figure 26. Pitch as measured by the Schaevitz inclinometer (triangles) from a trial with the arm rotating at 0.16 Hz and the table pitching at 0.31 Hz. Curves, dashes, and the line 0.61 s long have the same significance as in the previous figures.

It is apparent, though, that the data from this inclinometer do not agree with theoretical predictions as well as the data from the Humphrey inclinometer did. The discrepancy is due to the low resonant frequency and the damping constant. The Schaevitz inclinometer has a resonant frequency of 0.5 Hz, far closer to the frequencies of our apparatus than the 3.2-Hz frequency of the Humphrey inclinometer (all other sensors had even higher resonant frequencies). Undergraduate texts (Ref. 3) contain expressions for the amplitude of an harmonic motion of resonant frequency ω_o and damping time constant $1/\zeta$, driven at the frequency, ω. Let G be the ratio of the amplitude of this oscillator to one with $\omega << \omega_o$, then

$$G = \frac{\omega_o^2}{\left[(\omega_o^2 - \omega^2)^2 + 4\zeta^2\omega^2 \right]^{1/2}} \tag{12}$$

The time delay between the driving and resulting oscillations is

$$\tau = \frac{1}{\omega} \tan^{-1} \left[\frac{2\zeta\omega}{(\omega_o^2 - \omega^2)} \right] \tag{13}$$

For all the sensors except the Schaevitz inclinometer, G is within 1% of unity and τ < 30 ms. However this inclinometer has ω_o = 0.5 Hz and $1/\gamma$ = 0.3 s, which results in the gains and delays in Table 1. These values match the observed values quite well, with discrepancies likely due to inaccuracies in the manufacturer's values of ω_o and ζ. Thus we conclude that a sensor with resonant frequency as low as this is unsuited for sensing wave-driven motion.

TABLE 1

Gain and Time Delay of a Driven, Damped Oscillator and Comparison with Observations of the Schaevitz Inclinometer

Driving Frequency, ω (Hz)	Gain, G		Delay, τ (s) from Eq. 10
	Eq. 9	Observed	
0.11	0.93	0.94	0.72
0.21	0.79	0.87	0.67
0.31	0.66	0.79	0.61

Values calculated for a resonant frequency of 0.5 Hz and a damping time constant of 3.3 s. Observed delays were not calculated from the data, but the predicted delays are shown on each figure.

Schaevitz LSMP-2 Accelerometer

This accelerometer is typical of closed-loop force-balance accelerometers. The test mass, an unbalanced pendulum, is maintained very near its equilibrium position by a compensating electromagnetic torque, and the current which generates this torque also drives the output signal. The natural frequency is 131 Hz. The damping ratio, 0.71, is not important since the natural frequency far exceeds the driving frequency. Like most similar accelerometers, this unit is compact, reliable, and inexpensive.

Figures 27 and 28 show data from the accelerometer mounted to measure fore-aft acceleration on the yawing table, that is, with the table horizontal. The accelerometer results were converted to acceleration units using the manufacturer's calibration of 2.50 V/g. The theoretical curves in these figures are calculated, by macro "accs", from Equation 2, plus the

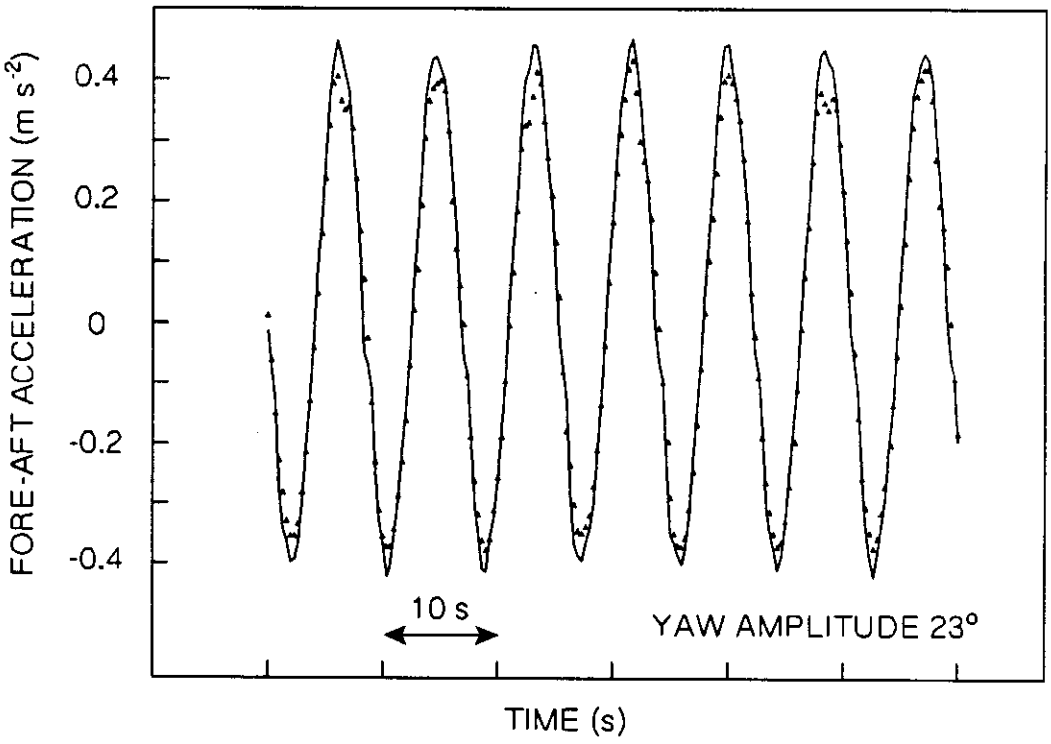

Figure 27. Fore-aft acceleration as measured by the Schaevitz accelerometer (triangles) from a trial with the arm rotating at 0.12 Hz and the table yawing at 0.31 Hz.

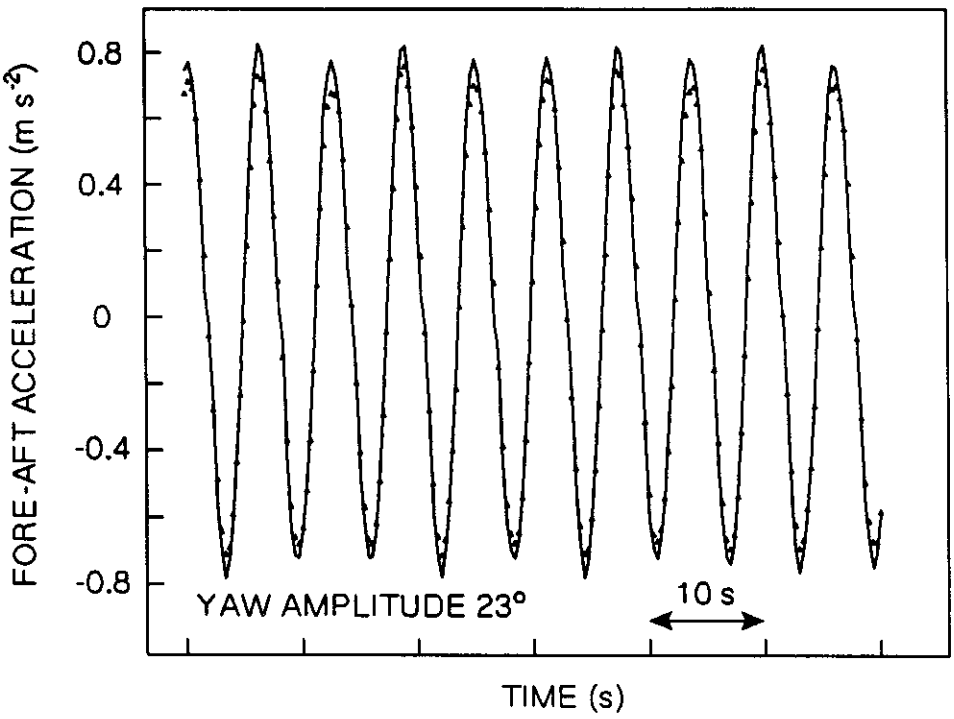

Figure 28. Fore-aft acceleration as measured by the Schaevitz accelerometer (triangles) from a trial with the arm rotating at 0.16 Hz and the table yawing at 0.20 Hz.

incidental effects. Equation 2 states that a good estimate of the acceleration is simply $-R\omega^2 \sin\theta \cos\phi$, which is close to a sinusoid since $\phi_{max} = 23°$. As always in this memorandum, the plotted curves also include the incidental effects. The most important incidental effect in this case is the incidental pitch, which ranges between 0.1° and 0.3° bow-down, and therefore subtracts between 0.05 and 0.01 m s^{-2} from the fore-aft acceleration. The accelerometer data agree reasonably well with the theoretical calculations, although it seems that the manufacturer's calibration is somewhat too small.

Figures 29 and 30 are quite different because a component of gravity is involved. They are from runs with the table vertical and pitching. The true fore-aft accelerations, as given (without incidental effects) by Equation 3, have amplitudes of 0.7 and 0.4 m s^{-2}. These are shown as the dashed curves across the middle of each figure. The major contribution to the fore-aft acceleration as seen by a strap-down

accelerometer is the component of gravity introduced by the pitch. The solid curve in each figure is the sum of the true acceleration and that gravitational component. On this scale, the instrument error and the calibration inaccuracies are barely visible, so the agreement between these curves and the measured data appears to be excellent. However the accelerometer result is clearly a very poor estimate of the true acceleration.

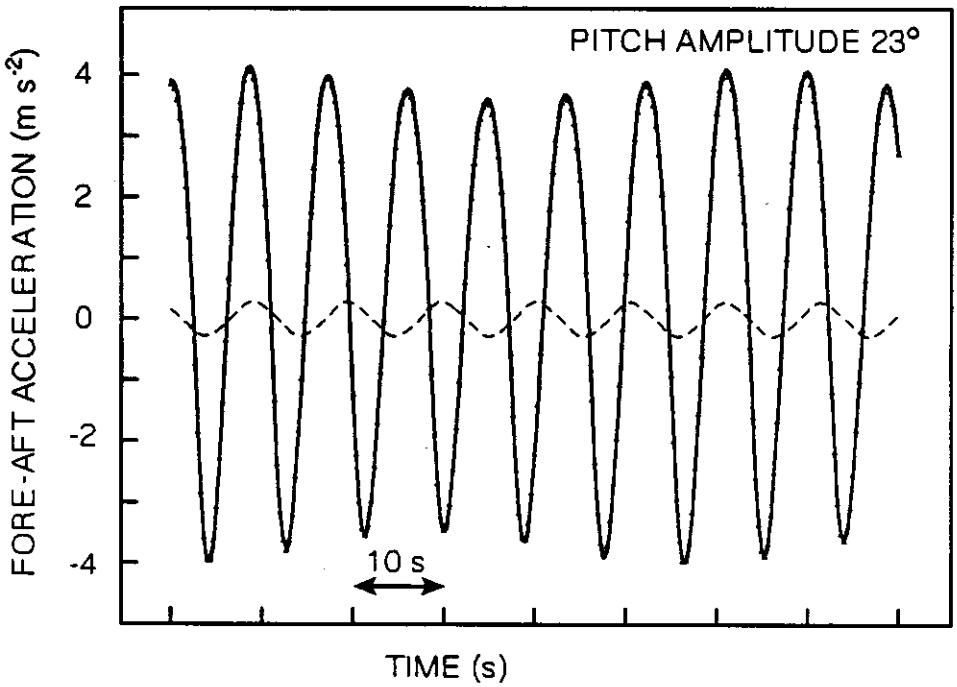

Figure 29. Fore-aft acceleration as measured by the Schaevitz accelerometer (triangles) from a trial with the arm rotating at 0.096 Hz and the table pitching at 0.32 Hz. The dashed curve is the true fore-aft acceleration of the table. The solid curve is the output one would expect from an accelerometer, which is dominated by the component of gravity which acts on the sensor due to its pitch.

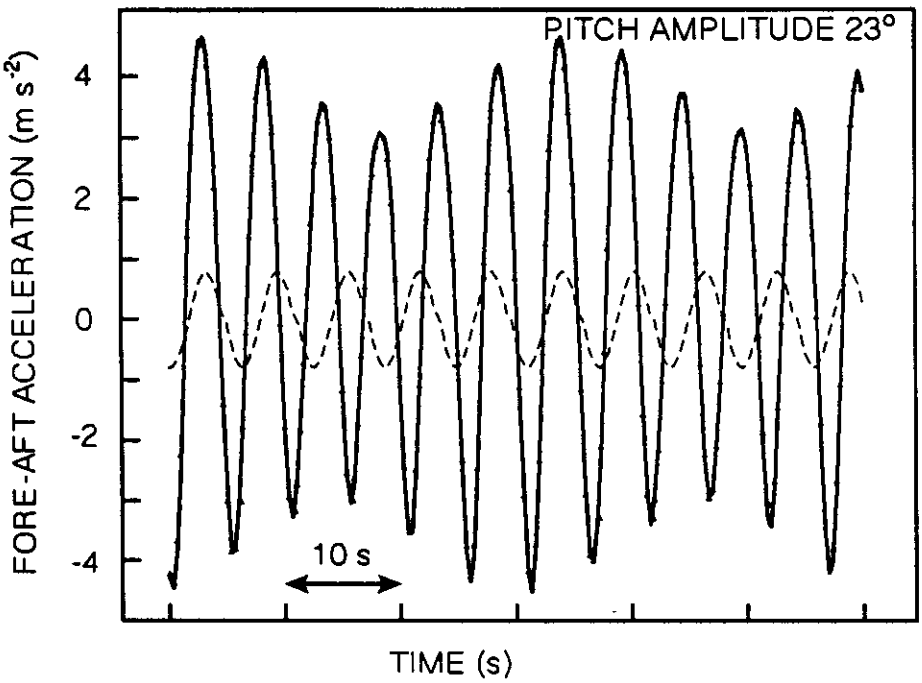

Figure 30. Fore-aft acceleration as measured by the Schaevitz accelerometer (triangles) from a trial with the arm rotating at 0.16 Hz and the table pitching at 0.20 Hz. The dashed curve is the true fore-aft acceleration of the table. The solid curve is the output one would expect from an accelerometer, which is dominated by the component of gravity which acts on the sensor due to its pitch.

Applications of Unstabilized Inclinometers and Accelerometers

Unstabilized inclinometers or accelerometers are, not infrequently, used to measure the pitch or roll of a marine vehicle. Examples in this memorandum have shown how the accelerations of a body can contaminate the output of an inclinometer mounted on it, and how roll or pitch of a body can contaminate the output of an accelerometer mounted on it. One might think that these contaminations could be removed if both types of instruments were used. However, in this section it will be shown that, to first order, unstabilized inclinometers and accelerometers measure the same thing, and thus that their outputs cannot be combined to derive acceleration and attitude.

Einstein's equivalence principle, the cornerstone of general relativity, states that the physical effects of a gravitational field are

indistinguishable from the physical effects of an accelerated coordinate system. On this basis, it can be shown that strapdown accelerometers and inclinometers measure the same combination of attitude and acceleration.

Consider an inclinometer aligned fore-aft on our pitching table, pitched by ϕ and with fore-aft and vertical accelerations $\ddot{y}$ and $\ddot{z}$. An inclinometer can be thought of as a pendulum constrained to move in a plane. It measures the angle between its internal reference direction and the equilibrium direction of the pendulum. If the body to which it is attached is not accelerating, the equilibrium direction is, of course, vertical. In general, though, following the equivalence principle, the angle measured, I, is

$$I = \phi + \tan^{-1}\left[\frac{\ddot{y}}{g + \ddot{z}}\right] \tag{13}$$

Our first-order approximation is that the acceleration components, $\ddot{y}$ and $\ddot{z}$, are much smaller than the gravitational acceleration, g, in which case

$$I = \phi + \frac{\ddot{y}}{g} \tag{14}$$

This, plus incidental effects, is the expression used to calculate expected inclinometer responses in this memorandum, and good agreement with measurements was noted.

Now replace the inclinometer with an accelerometer, again aligned fore-aft along the sensor. Its output, A, is the fore-aft component of the vector sum of the body's acceleration, $\underline{a}$, and gravity.

$$A = (\underline{a} + g)\cdot\hat{f} = \ddot{y}\cos\phi + (\ddot{z} + g)\sin\phi \tag{15}$$

where $\hat{f}$ is a fore-aft unit vector. With the same first-order approximation, we have

$$A = \ddot{y} + g\phi \tag{16}$$

This, plus incidental effects, is the expression used to calculate expected accelerometer responses in this memorandum, and good agreement with measurements was noted.

The identical argument can be made for an inclinometer which measures roll and a transverse accelerometer. Thus we see that gI and A are two measures of the same quantity.

The use of unstabilized accelerometers or inclinometers has been shown, by the examples above, to give measurements of attitude or acceleration which can be significantly contaminated, the one by the other. Furthermore, in this section it has been shown that it is not possible to use one instrument to correct the contaminated output of the other, as they both measure the same quantity.

CONCLUSIONS

This apparatus has been shown to be an effective means of testing sensors which measure the acceleration or attitude of marine vehicles. The use of two drive frequencies, one for the rotating arm and one for the yawing or pitching sensor table, was shown to be an advantage in separating the effects of these two motions. The range of accelerations and frequencies is representative of both the routine and the more demanding applications for such sensors. Incidental motions of the rig have been carefully modelled and can be used to assess appropriate performance limits of quite sensitive sensors. However, this apparatus was not intended to provide highly precise calibration of the most sophisticated instruments.

The Humphrey gyroscopically stabilized package has been shown to be an appropriate baseline instrument for measuring wave-driven motions. Its sensitivity, resolution, and resonant frequencies are well suited to these motions.

The Watson angular-rate sensor was found to provide excellent performance from an affordable compact package. Rejection of linear accelerations was found to be essentially complete. This sensor merits further investigation for body-motion applications.

The two inclinometers were found to be quite accurate. However two problems were highlighted in this investigation. First, if the resonant frequency of the sensor is not significantly higher than the wave-driven motions, undesirable attenuation and delays can occur. These effects make the Schaevitz inclinometer unsuitable for many ocean-wave-driven applications. Second, but more fundamental, it was clearly shown that the acceleration of the body can contaminate significantly measurements of pitch or roll by any inclinometer.

The Humphrey accelerometer was also shown to be highly accurate. However several examples clearly demonstrated that an inclination of the body can significantly contaminate the acceleration measurements. In our examples, the pitch angles were large and the accelerations fairly modest, and thus the gravitational component introduced by the pitch actually exceeded the true acceleration.

The interaction of inclination and acceleration in the outputs from strapdown inclinometers and accelerometers highlight the technology used to eliminate undesirable effects. Mechanical gyroscopic stabilization is the established technique, as exemplified by our Humphrey package. This technique ensures that the accelerometers are always in a vertically referenced frame, and the angles between that frame and the case of the instrument can be measured to provide pitch and roll. The developing technology is the independent measurement of pitch and roll, and the use of that information to correct the outputs of a triad of strapdown accelerometers. While much attention has been focussed on ring-laser and optical-fibre gyros for the angular measurements, by integration of angular rates, these instruments would be very expensive. Thus there is growing interest in angular-rate sensors such as the Watson sensor evaluated here, for this application.

BIBLIOGRAPHY

1. "Stability of Towfish as Sonar Platforms and Benefits of the Two-Part Tow", J.M. Preston, Defence Research Establishment Pacific Technical Memorandum 89-19 (1989).

2. "Effect of Ship Motion on a Neutrally-Stable Towed Fish", D.A. Chapman. Ocean Engng, 9 189-220 (1982).

3. See, for example, "Analytical Mechanics", G.R. Fowles, Holt, Rinehart and Winston (1962).

APPENDIX A

Macros

The following macros, written in the MAGnetics Interactive Graphics package, MAGIC, were used to convert data from all the sensors to physical units, to calculate the accelerations and attitudes of the table, and to plot the results. Note that all possible accelerations and attitudes were calculated, and the user was responsible for selecting the correct data set for comparision with the sensor.

```
macro expt plate sensor
continue                          Macro expt plate sensor
continue                        Plate: 1=horiz  0=vert
continue                        Sensor: 1=gyro pack  0=small units
continue
continue                        Angles:    Horiz table       Vert table
ap00 = 0                                  mean   amp  phase   mean  amp  phase
ap0 = 0.0082                       yaw      0   .0082  114      0  .0082  114
thap = 114                         rol   -.0011 .0106 -171   .0026 .0106 -171
be00 = -0.0011                     pit   -.0033 .0020  -21  -.0028 .0020  -21
be0 = 0.0106                          (mean & amp in radians, phase in deg)
thbe = -171
ga00 = -0.0033                   Offsets:  Horiz table        Vert table
ga0 = 0.0020                             Gyro    Small      Gyro   Small
thga = -21                         rx      .148    .148       .175    .147
rx = 0.148                         rz      .020   -.050      -.112   -.112
rz = 0.020                            (in metres, rx positive in neg x direction)
if plate*sensor exit a exit
a: rz = -0.005
if sensor exit v exit
v: be00 = 0.0026
ga00 = -0.0028
rx = 0.175
rz = -0.112
if sensor exit b exit
b: rx = 0.147
end expt
```

```
macro readrig
point 1 2048 1 1
readi2,2,'phi.mg2'        Regr fit: Dig. out = 16803.56 - 46.346*phi
examine,2,,,,,num
num=num-1
point 1 num 1 1
addc 2 -1280.9 2          Yaw for least la_ac = 334.93.  16803-46.346*334=-1281
multc 2 0.021577 2        1/46.346 = 0.021577       Bow to starboard positive
read,64,'limfr'
point 1 1 1 1
examine 64 limit
point 1 num 1 1
readi2,1,'roti.mg2'
multc 1 -360/limit 1      Limit = 4024 before 22 Mar, 4092 after
addc 1 360 1
shift 1 2 1 1             Rot not filtered.  All others delayed 2/3 s
readi2,51,'pit.mg2'       Nose-up positive
addc 51 61.6 51
multc 51 -0.01433 51
readi2,52,'roll.mg2'      Starboard-up positive
addc 52 -25.43 52
multc 52 -0.0306 52
readi2,53,'faac.mg2'      Forward positive
addc 53 3.9 53
multc 53 0.00143 53       Mean set to zero
examine 53  mean
addc 53 -1*mean 53
readi2,54,'laac.mg2'      To starboard positive
addc 54 59.6 54
multc 54 0.00141 54       Mean set to zero
examine 54 mean
addc 54 -1*mean 54
readi2,56,'vacc.mg2'      Up positive
```

```
examine 56 mean
addc 56 -1*mean 56        Mean set to -g
multc 56 0.00283 56
addc 56 g 56
read,63,'acoeff'
read,64,'bcoeff'
point 1 8
frar 63 a
frar 64 b
point 3 num
setto 1 num/3
end readrig


macro accs freq
continue          Calculate accs and attitude of table.  Required variables:
freqsq=freq*freq       freq in rad/s = 6*pie*(cycles)/(points)
continue               ap00, ap0, thap   (alpha=ap00+ap0*sin(theta-thap)) yaw
g = 9.8062             be00, be0, thbe   (beta=be00+be0*sin(theta-thbe))  roll
rbig=0.7523            ga00, ga0, thga   (gamma=ga00+ga0*sin(theta-thga)) pitch
point 3 num       Frame Assignments
continue            1: Rot=theta  2: Phi (yaw for horiz table, pitch for vert)
continue            3: alpha (rad)  4: alpha (deg)
continue            5: phi + alpha (deg)  6: phi + gamma (deg)
continue            8: d(phi)/dt (radians/s)   9: d(phi)/dt (degrees/s)
continue            10: sin(theta)  11: cos(theta)
continue            12: gamma (radians)  13: beta (radians)
continue            14: rbig freqsq sin(theta)
continue            15: rbig freqsq cos(theta)
continue            16: gamma (deg)  17: beta (deg)
continue            18: freqsq rx ap0 sin(theta-thap)
continue            19  freqsq rx be0 sin(theta-thbe)
continue            20: freqsq rz be0 sin(theta-thbe)  22: fseries
continue            21: freqsq rz ga0 sin(theta-thga)  23: fnseries
continue            24: -14 - twice*14*22 + 15*23 - 18 + 21
continue            25: -15 - twice*15*22 - 14*23 + 19
continue            26: 20*cos(5) - 24*sin(5)  [la_ac] (gy)
continue            27: 24*cos(5) + 20*sin(5)  [fa_ac] (gy)
continue            28: 16*cos(5) + 17*sin(5)  [pitch]  [ ] means in sensor's
continue            29: 17*cos(5) - 16*sin(5)  [roll]   frame with yawing table
continue            30: 25 - g          [ve_ac] & (ve_ac) (gy)
continue            31: 30 - 12*24      [ve_ac] (no gy)
continue            32: 27 - 12*30      [fa_ac] (no gy)
continue            33: 26 - 13*30      [la_ac] (no gy)    ( ) means in sensor's
continue            34: 24 + 3*20       (fa_ac) (gy)       frame with pitch table
continue            35: 20 + 3*24       (la_ac) (gy)
continue            36: 34*cos(6) + 30*sin(6) (fa_ac) (no gy)
continue            37: 35 - 13*30            (la_ac) (no gy)
continue            38: 30*cos(6) - 24*sin(6) (ve_ac) (no gy)
continue            39: 4*cos(6) - 17*sin(6)  (yaw)
continue            40: 6 + 180/pie*34/g      (inclinometer)
sinfr 1 10 1              d2x/dt2 in frame 20         [yaw] in frame 5
cosfr 1 11 1              d2y/dt2 in frame 24         (pitch) in frame 6
addc 1 -1*thga 12         d2z/dt2 in frame 25         (roll) in frame 17
sinfr 12 12 1
multc 12 ga0 12
move 12 21
addc 12 ga00 12
multc 12 180/pie 16
add 2 16 6
addc 1 -1*thbe 13
sinfr 13 13 1
multc 13 be0 13
move 13 19
move 13 20
addc 13 be00 13
multc 13 180/pie 17
move 10 14
multc 14 freqsq*rbig 14
move 11 15
multc 15 freqsq*rbig 15
addc 1 -1*thap 18
sinfr 18 18 1
multc 18 ap0 3
multc 3 180/pie 4
add 2 4 5
multc  3 freqsq*rx 18
multc 19 freqsq*rx 19
multc 20 freqsq*rz 20
multc 21 freqsq*rz 21
fseries 1 26 22
fnseries 1 26 23
mult 14 22 24
multc 24 -2 24
mult 15 23 26
add 24 26 24
sub 24 14 24
```

```
sub 24 18 24
add 24 21 24
mult 15 22 25
multc 25 -2 25
mult 14 23 26
sub 25 26 25
sub 25 15 25
add 25 19 25
sinfr 5 8 1
cosfr 5 9 1
mult 20 9 26
mult 24 8 27
sub 26 27 26
mult 20 8 27
mult 24 9 28
add 27 28 27
mult 16 9 28
mult 17 8 29
add 28 29 28
mult 17 9 29
mult 16 8 8
sub 29 8 29
derivx 2 9
multc 9 3 9
sinfr 6 8 1
cosfr 6 7 1
addc 25 g 30
mult 12 24 31
sub 30 31 31
mult 12 30 32
sub 27 32 32
mult 13 30 33
sub 26 33 33
mult 3 20 34
add 24 34 34
mult 3 24 35
add 20 35 35
mult 34 7 36
mult 30 8 37
add 36 37 36
mult 30 7 38
mult 24 6 37
sub 38 37 38
mult 4 7 39
mult 17 8 37
sub 39 37 39
mult 13 30 37
sub 35 37 37
multc 9 pie/180 8
multc 34 180/pie/g 40
add 40 6 40
pretty
point 5 num
setto 2 num/3
end accs


macro watson
point 1 2048 1 1
readi2,2,'phi.mg2'          Regr fit: Dig. out = 16803.56 - 46.346*phi
examine,2,,,,,num
num=num-1
point 1 num 1 1
addc 2 -1280.9 2             Yaw for least la_ac = 334.93.  16803-46.346*334=-1281
multc 2 0.021577 2           1/46.346 = 0.021577       Bow to starboard positive
readi2,1,'roti.mg2'
multc 1 -360/4092 1          For trials after 22 Mar, use 4092, not 4024
addc 1 360 1
shift 1 2 1 1                Rot not filtered.  All others delayed 2/3 s
readi2,51,'rate.mg2'
addc 51 -36 51               Offset of filter/amplifier
multc 51 -0.007413 51        Analog gain 0.494, A/D 5V=4096, 3 deg/s/V
read,63,'acoeff'
read,64,'bcoeff'
point 1 8
frar 63 a
frar 64 b
point 3 num
setto 1 num/3
end watson


macro schinc
point 1 2048 1 1
readi2,2,'phi.mg2'           Regr fit: Dig. out = 16803.56 - 46.346*phi
examine,2,,,,,num                      phi = 362.54 - Dig./46.346
num=num-1
```

```
point 1 num 1 1
multc 2 1/46.346 2          Pitch = 336.60 - phi = Dig./46.346 - 25.94
addc 2 -25.94 2
readi2,1,'roti.mg2'
multc 1 -360/4092 1         For trials after 22 Mar, use 4092, not 4024
addc 1 360 1
shift 1 2 1 1               Rot not filtered.  All others delayed 2/3 s
readi2,51,'inc.mg2'
addc 51 342 51              Offset of fil/amp is -148.  Offset of inc about 490
multc 51 0.009958 51        Analog gain 2.043, A/D 5V=4096, 60 mV/deg
read,63,'acoeff'
read,64,'bcoeff'
point 1 8
frar 63 a
frar 64 b
point 3 num
setto 1 num/3
end inclin


macro huminc
point 1 2048 1 1
readi2,2,'phi.mg2'          Regr fit: Dig. out = 16803.56 - 46.346*phi
examine,2,,,,,num                     phi = 362.54 - Dig./46.346
num=num-1
point 1 num 1 1
multc 2 1/46.346 2          Pitch = 336.60 - phi = Dig./46.346 - 25.94
addc 2 -25.94 2
readi2,1,'roti.mg2'
multc 1 -360/4092 1         For trials after 22 Mar, use 4092, not 4024
addc 1 360 1
shift 1 2 1 1               Rot not filtered.  All others delayed 2/3 s
readi2,51,'inc.mg2'
addc 51 -36 51              Offset of filter/amplifier
multc 51 -0.01483 51        Analog gain 0.494, A/D 5V=4096, 15 V for 90 deg
read,63,'acoeff'
read,64,'bcoeff'
point 1 8
frar 63 a
frar 64 b
point 3 num
setto 1 num/3
end inclin


macro schacc
point 1 2048 1 1
readi2,2,'phi.mg2'          Regr fit: Dig. out = 16803.56 - 46.346*phi
examine,2,,,,,num
num=num-1
point 1 num 1 1
multc 2 1/46.346 2          Pitch or yaw = 336.65 - phi = Dig./46.346 - 25.91
addc 2 -25.91 2
readi2,1,'roti.mg2'
multc 1 -360/4092 1         For trials after 22 Mar, use 4092, not 4024
addc 1 360 1
shift 1 2 1 1               Rot not filtered.  All others delayed 2/3 s
readi2,51,'faac.mg2'
addc 51 -148 51             Offset of filter/amplifier
multc 51 0.002346 51        Analog gain 2.043, A/D 5V=4096, 255 mV/(m/s2)
read,63,'acoeff'
read,64,'bcoeff'
point 1 8
frar 63 a
frar 64 b
point 3 num
setto 1 num/3
end schacc
```

```
macro fseries thetafr workfr outfr      unitless
move thetafr outfr                      (w-w_o)/w_o
multc outfr 0 outfr
do a1 n 1 8
multc thetafr n workfr
sinfr workfr workfr+1 1
multc workfr+1 a(n) workfr+1
add workfr+1 outfr outfr
cosfr workfr workfr+2 1
multc workfr+2 b(n) workfr+2
a1: add workfr+2 outfr outfr
end fseries
```

```
macro fnseries thetafr workfr outfr     1/rad
move thetafr outfr                      w(dw/dtheta)/w_o^2
multc outfr 0 outfr
do a1 n 1 8
multc thetafr n workfr
sinfr workfr workfr+1 1
multc workfr+1 -1*n*b(n) workfr+1
add workfr+1 outfr outfr
cosfr workfr workfr+2 1
multc workfr+2 n*a(n) workfr+2
a1: add workfr+2 outfr outfr
end fnseries
```

DISTRIBUTION LIST

"EVALUATION OF ATTITUDE AND ACCELERATION SENSORS FOR MARINE APPLICATIONS"

NDHQ and Maritime Command:

__	DSIS
1	CRAD/DRDM
1	DREA
1	DREA Attn: Jim Colwell
1	DGRD/Ops
1	RRMC Library
1	DNR-7
1	DMCS-3
1	DMES-3
1	PM NRMP

Internal:

10	DREP Library
1	H/Electromagnetics
1	H/Applied Technology
1	Group Leader, Mine Countermeasures, (Dr. R.H. Kuwahara)
1	Dr. J.M. Preston
1	Dr. W.M. Vogel
1	Ms. S.A. Latchman
1	Mr. D. Hopkin
1	Mr. A. Fitchett
1	Mr. R. Chappell
1	Mr. D. Schneider

TTCP/GTP-13 and International:

1 Materials Research Laboratories
Underwater Weapons and Countermeasures Division
MRL Melbourne
P.O. Box 50, Ascot Vale
Victoria 3032, Australia
Attn: G. Campanella

1 Admiralty Research Establishment
Southwell, Portland, Dorset
England, DT5 2JS
Attn: R. Breward

Canadian Industry:

1 Offshore Systems Ltd.
1974 Spicer Road,
North Vancouver, BC V7H 1A2
Attn: Mr. H. Lanzinger

1 Simrad Mesotech
2830 Huntington Place
Port Coquitlam, BC V3C 4T3
Attn: Dr. P. Fox

1 International Submarine Engineering Ltd.
1734 Broadway St.
Port Coquitlam, BC V3C 2M8
Attn: Mr. J.S. Ferguson

1 MacDonald Dettwiler Associates Ltd.
3751 Shell Road
Richmond, BC V6X 2Z9
Attn: Mr. D. Molnar

1 GeoAcoustics Ltd.
Box 772
Aurora, Ont L4G 4J9
Attn: Mr. J. Dodds

1 C-Tech Ltd
PO Box 1960
Cornwall, Ont K6H 6N7
Attn: Mr. H.M. Johnson

1 MEL Defence Systems
1 Iber Road
Stittsville, Ont K2S 1E6
Attn: Mr. P. Johnson

(NON-CONTROLLED GOODS)
DMC A

DOCUMENT CONTROL DATA

(Security classification of title, body of abstract and indexing annotation must be entered when the overall document is classified)

1. ORIGINATOR (the name and address of the organization preparing the document. Organizations for whom the document was prepared, e.g. Establishment sponsoring a contractor's report, or tasking agency, are entered in section 8.)

Defence Research Establishment Pacific
FMO Victoria, B. C.
VOS 1BO

2. SECURITY CLASSIFICATION (overall security classification of the document. including special warning terms if applicable)

UNCLASSIFIED

3. TITLE (the complete document title as indicated on the title page. Its classification should be indicated by the appropriate abbreviation (S,C or U) in parentheses after the title.)

Evaluation of Attitude and Acceleration Sensors for Marine Applications

4. AUTHORS (Last name, first name, middle initial)

Preston, Jonathan M.

5. DATE OF PUBLICATION (month and year of publication of document)

Sep 90

6a. NO. OF PAGES (total containing information. Include Annexes, Appendices, etc.)

6b. NO. OF REFS (total cited in document)

3

7. DESCRIPTIVE NOTES (the category of the document, e.g. technical report, technical note or memorandum. If appropriate, enter the type of report, e.g. interim, progress, summary, annual or final. Give the inclusive dates when a specific reporting period is covered.)

Technical Memorandum

8. SPONSORING ACTIVITY (the name of the department project office or laboratory sponsoring the research and development. Include the address.)

9a. PROJECT OR GRANT NO. (if appropriate, the applicable research and development project or grant number under which the document was written. Please specify whether project or grant)

9b. CONTRACT NO. (if appropriate, the applicable number under which the document was written)

10a. ORIGINATOR'S DOCUMENT NUMBER (the official document number by which the document is identified by the originating activity. This number must be unique to this document.)

10b. OTHER DOCUMENT NOS. (Any other numbers which may be assigned this document either by the originator or by the sponsor)

11. DOCUMENT AVAILABILITY (any limitations on further dissemination of the document, other than those imposed by security classification)

(X) Unlimited distribution
( ) Distribution limited to defence departments and defence contractors; further distribution only as approved
( ) Distribution limited to defence departments and Canadian defence contractors; further distribution only as approved
( ) Distribution limited to government departments and agencies; further distribution only as approved
( ) Distribution limited to defence departments; further distribution only as approved
( ) Other (please specify):

12. DOCUMENT ANNOUNCEMENT (any limitation to the bibliographic announcement of this document. This will normally correspond to the Document Availability (11). However, where further distribution (beyond the audience specified in 11) is possible, a wider announcement audience may be selected.)

13. ABSTRACT (a brief and factual summary of the document. It may also appear elsewhere in the body of the document itself. It is highly desirable that the abstract of classified documents be unclassified. Each paragraph of the abstract shall begin with an indication of the security classification of the information in the paragraph (unless the document itself is unclassified) represented as (S), (C), or (U). It is not necessary to include here abstracts in both offical languages unless the text is bilingual).

A wide variety of instruments are available for measuring the attitude and accelerations of a marine vehicle, with characteristic advantages and limitations. The apparatus described here was built to evaluate such sensors against accurately measured accelerations and attitudes. It resembles a small Ferris wheel, and moves the sensor on 1.5-m diameter circles, on a support which remains horizontal, at selectable frequencies similar to those of ocean waves. The sensor can be yawed or pitched, asynchronously with the rotation. The acceleration and attitude of the sensor can be calculated from the shaft encoders on the rotation and yaw/pitch axles. Results are given for two inclinometers, an accelerometer, a piezoelectric angular-rate sensor, and a gyroscopically stabilized accelerometer package.

14. KEYWORDS, DESCRIPTORS or IDENTIFIERS (technically meaningful terms or short phrases that characterize a document and could be helpful in cataloguing the document. They should be selected so that no security classification is required. Identifiers, such as equipment model designation, trade name, military project code name, geographic location may also be included. If possible keywords should be selected from a published thesaurus, e.g. Thesaurus of Engineering and Scientific Terms (TEST) and that thesaurus-identified. If it is not possible to select indexing terms which are Unclassified, the classification of each should be indicated as with the title.)

Acceleration measurement

Accelerometers

Attitude indicators

Attitude (inclination)

Inclinometers

Vertical indicators

(all terms are from TEST)